Curdlan 1,3-Beta-Glucans: A New Platform for Polymer Drug Delivery

by

Benjamin C. Lehtovaara

A thesis

presented to the University of Waterloo

in fulfillment of the

thesis requirement for the degree of

Master of Applied Science

in

Chemical Engineering

Waterloo, Ontario, Canada, 2011

© Benjamin C. Lehtovaara 2011

Author's Declaration

I hereby declare that I am the sole author of this thesis. This is a true copy of the thesis, including any required final revisions, as accepted by my examiners.

I understand that my thesis may be made electronically available to the public.

Abstract

1,3-β-glucans are a class of natural polysaccharides with unique pharmacological properties and the ability to form triple helical structures and resilient gels. Curdlan and other 1,3-β-glucans have found application pharmacologically in the treatment of cancers and acceleration of wound healing in humans and in the impartation of infection resistance in animal husbandry. Structurally, these polysaccharides have found application in food science as thermal gels, in nanostructure formation as helical scaffolds, and in drug delivery as nanocarriers for drugs and as inclusion complexes with polynucleotides.

A literature review of the important work on Curdlan research reveals two streams of research: investigation of the pharmacological significance of these polymers and their application in increasing host immunocompetency and investigation of the nature of the triple helix and its application in a variety of fields from food gels to drug delivery. Two significant contributions to the field of Curdlan research have been completed including 1) The development of a Curdlan nanoparticle drug delivery platform and 2) A new multi-component liquid crystalline hydrogel providing a new route to form polynucleotide inclusion complexes with Curdlan for gene delivery. The developed nanoparticle platform exhibited high encapsulation of chemotherapeutic drugs and a 24-hour controlled release with a particle size of 109.9 nm. The liquid crystalline hydrogel exhibited homogeneous inclusion of DNA into amorphous and crystalline phases of Curdlan and delayed and triggered release of polynucleotide content. This work has been a significant demonstration of the potential of Curdlan as a new polymer for multi-functional drug delivery.

Acknowledgements

I would like to acknowledge the exceptional guidance of my supervisor, Dr. Frank Gu for his consistent contribution of ideas that made this work successful. I want to give special thanks to Mohit Verma for his collaboration on the work on liquid crystalline gels and must acknowledge Jan Venne and Dale Weber for their valuable expertise on spectroscopic techniques and electron microscopy equipment.

This thesis is dedicated to:

My grandfather, Bill, who lost his life to cancer during the course of my studies

and

My wife, Janice, who provided love and support during the course of my education

Table of Contents

List of Tables

List of Illustrations

1.0 General Introduction

Modern drug delivery techniques seek to alter the pharmacokinetics and pharmacodynamics of drug substances such as pharmaceuticals, chemotherapeutics, peptides, or genes (polynucleotides) in the human body. Modulation of pharmacokinetics targets the absorption, distribution, metabolism, and elimination of drug substances in the body and modulation of pharmacodynamics alters the uptake of drugs into cells and the overall effect of the drug substance.

Alteration to the absorption, distribution, metabolism, and elimination (ADME) of a drug substance is most often accomplished using controlled release technologies. These technologies typically utilize encapsulation by a biocompatible substance that acts as a diffusional barrier to provide controlled release, degrades over time to provide delayed release, or has a specific triggered mechanism of degradation to provide triggered release. Modulation of pharmacodynamics typically alters the interactions occurring between the drug substance and the body. In terms of the extent of interactions, drug delivery systems seek to ensure that drug interactions with the body occur only at the intended site of action, reducing side effects and patient suffering. For example, in the case of chemotherapy, systemic distribution of chemotherapeutics results in widespread destruction of fast-growing cells including cancer cells, immune cells, and hair follicles causing devastating side effects. Drug delivery systems typically reduce unintended drug interactions through encapsulation of the substance and the use of targeting mechanisms such as receptor-ligand interactions to ensure the drug payload is delivered to the intended site. In terms of cellular uptake, the use of a targeting mechanism in a receptor-ligand relationship can improve the cellular uptake of a substance. Simultaneous delivery of an

adjuvant substance to boost the cellular uptake of the drug is also an popular approach, especially in the case of delivery of adjuvants to boost the effect of vaccines.

This thesis describes work done in the development of polymer nanoparticle drug delivery system and a polymer hydrogel gene delivery system. These two examples of drug delivery systems are described next as a general introduction.

1.1 Polymer Nanoparticle Delivery Systems

Drug delivery systems have a number of manifestations that seek to accomplish the goals of improving pharmacokinetics and pharmacodynamics. Polymer nanoparticle drug delivery systems use nanocapsules to alter the pharmacokinetics and pharmacodynamics of a drug substance by providing a biocompatible polymer coating that affords controlled release and restricts unintended exposure to the body[1]. Copolymer nanoparticle systems are especially popular as they utilize the self-assembly of an amphiphilic copolymer to form core-shell micelles wherein the internal core is typically hydrophobic and the outer shell in hydrophilic. Since many drug substances are hydrophobic and proteins in the body show less adsorbance on hydrophilic surfaces, the system acts as an ideal nanocapsule that holds a drug payload in its core and provides a 'stealth' effect from the immune system. Furthermore, the size of polymer micelles are typically less than 200 nm, affording the use of the enhanced permeability and retention effect (EPR) that allows targeting of leaky tumor vasculature by size alone without the need for a targeting mechanism[2, 3]. A number of literature reviews exist of trends in polymer nanoparticle drug delivery[1, 4-7].

1.2 Hydrogel Drug Delivery Systems

Hydrogel systems are typically cross-linked polymer networks that entrap drug substances amongst their fibers and provide controlled release through network swelling and

contraction or dissolution of cross-links in response to external stimuli such as pH or temperature. These systems are particularly attractive as they often use hydrophilic polymers that allow water swelling, providing excellent biocompatibility. Hydrogels may be formed into nanoparticles and used in systemic distribution as with other polymer nanoparticle systems[8] but they also provide unique applications in oral drug delivery due to their pH sensitivity and in the direct injection into sites of action due to their temperature sensitivity[9]. For example, direct injection into joints affords a temperature change from ambient room temperature to body temperature of 37 °C that can result in gel swelling to release drug substances packed into the fibrous network or alternatively yield gel contraction to provide a controlled release effect as the hydrogel degrades. Polysaccharides such as alginates that cross-link with calcium ions to form hydrogels have been studied extensively for drug delivery applications[10].

1.3 Natural Polysaccharides with Biomedical Properties

Natural polysaccharides are an especially promising research direction in polymer drug delivery and biomedical applications because they are so abundant in nature, are often naturally biocompatible, and they typically provide additional properties that aren't attainable from synthetic polymers. Notable examples are cellulose from wood or bacterial sources now used in novel bandage materials to speed wound healing[11], chitosan from shrimp shells with mucoadhesive properties that can facilitate ocular drug delivery[12, 13], and alginates from kelp that form hydrogels suitable as scaffolds for model extracellular matrices[14]or protein delivery vehicles that avoid protein denaturation during gelation[10].

1.4 The Family of 1,3-Beta-Glucans and Curdlan

1,3-β-glucans are a class of glucopyranose polysaccharides with (1,3) glycosidic linkages (Fig 1) and varying degrees of (1,6) branching obtained from fungal[15] or microbial sources[16]. An

illustration of the fungal cell wall adapted from electron micrographs of *Candida Albicans*[17] demonstrates the natural presence of β-glucans in fungi (Fig 2). 1,3-β-glucans form helical structures that may be prompted to gel with the addition of heat and have a unique ability to increase host immunocompetency. Reported pharmacological effects include anti-tumor activity[18-20], infection resistance[21, 22], and wound healing[23-25].

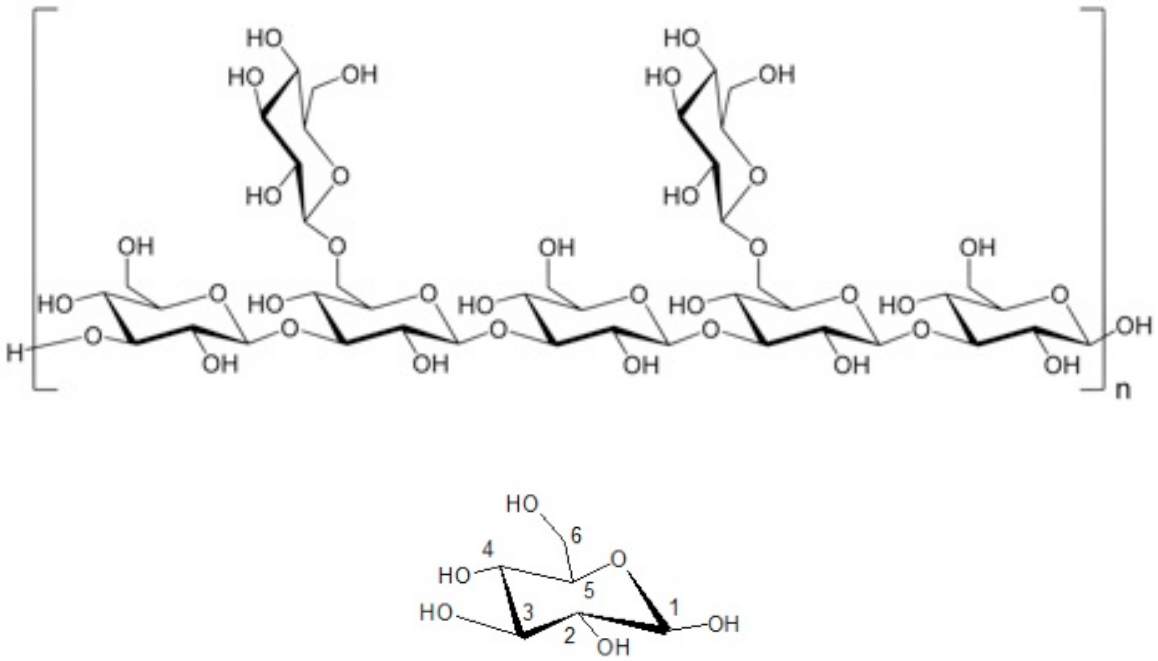

Figure 1. Schematic of a 1,3-Beta-Glucan. (Top) Schematic of 1,3-β-glucans consisting of glucopyranose monomers joined by glycosydic ether linkages between C(1) and C(3) in the glucopyranose rings and branch points often occur periodical in the (1,6) configuration. **(Bottom)** Numbering of carbons in glucose.

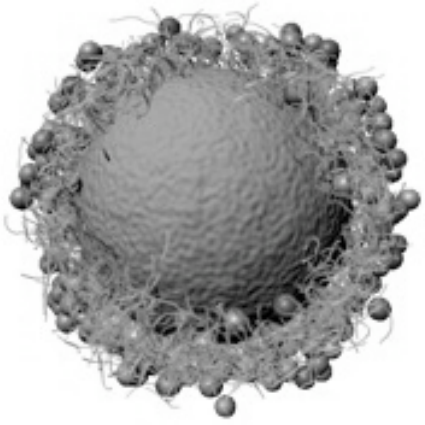

Figure 2. Schematic of a Fungal Cell Wall[17]**.** Adapted schematic of the fungal cell wall containing a composite of chitin and β-glucans with interspersed mannoproteins (spheres) surrounding the phospholipid membrane.

The formation of 1,3-β-glucan helical domains may be utilized for many applications or, as the helices natural cross-link through hydrogen bonding, be allowed to continue to the formation of a hydrogel network. The gelation profile is dependent on the degree of branching due to the effect of C(6) branching on helix packing[26]. Curdlan, a linear 1,3-β-glucan, has been used as a good model for the study of 1,3-β-glucan helical structures as it lacks the interference of periodic branching[27, 28]. The unique properties of 1,3-β-glucans have led to a variety of applications including the formulation of food gels for consumption or to improve stability and nutrition[29, 30], direct therapeutic application[31, 32], encapsulation and controlled release of various bioactive species[33, 34], and application as helical scaffolds for nanostructure formation[35, 36].

This thesis focuses on the demonstration of Curdlan 1,3-beta-glucans as a new platform for polymer drug delivery. Before establishing specific objectives for contributions to the literature, a comprehensive literature review is provided. This review begins with a discussion of the physical properties and gelation capabilities of 1,3-beta-glucans, using Curdlan as the primary example as has been the trend in the literature due to its lack of interfering branching effects. The review then describes the bioactivity of 1,3-beta-glucans as a whole and reviews all the relevant applications that have been developed using this family of polysaccharides.

2.0 Literature Review

2.1 Physical Properties of Curdlan 1,3-β-glucans

Curdlan was first discovered as a resilient gel forming polysaccharide bearing β-glycosydic linkages that was biosynthesized from the soil bacterium *Alcaligenes faecalis var. myxogenes* in the mid-1960's[37, 38]. Curdlan was found to be a linear 1,3-β-glucan that was insoluble in water but soluble in alkaline solutions. Experimentation with the gelation characteristics of Curdlan began shortly afterwards[39, 40]. Alkaline solutions inhibit hydrogen bonding between C(2) hydroxyls, inhibiting helix formation, leaving the random coil state. Commercial alkali treatment leaves most available Curdlan powder < 30% crystalline with a prevalence of a mixture of random coils and some single and triple helices[41]. This partially crystalline native form may be thermally treated in water to induce hydrogen bonded crystallinity and the incorporation of water molecules into helical structures to form a hydrogel. This hydrated, crystallized form may then be dehydrated to further improve crystallinity and re-swelled at will.

2.1.1 Helical Conformations in Curdlan

Helical polysaccharide structures held together by O(2) hydrogen bonding in 1,3-linked polysaccharides were hypothesized in 1968[42]. As stated previously, Curdlan may form both single helical and triple helical structures with some disagreement in the literature as to the relative populations of these species[43]. Single helices form via intra-chain hydrogen bonding between O(2) hydroxyls on glucopyranose residues[44]. Gelation of Curdlan causes single helices to rearrange hydrogen bonds to form inter-strand hydrogen bonding and hence the formation of the triple helix.

X-ray Diffraction uncovered the first evidence of the triple helical structures in gelled and dehydrated Curdlan. A right-handed triple helical model was assigned with six glucose residues per turn and a monomer advance of 2.935 Å (Fig 3; top) [27]. A model projection of the Curdlan triple helix is shown in (Fig 3b; top) with the six glucose residues (two from each single helix) in each turn[44]. The periodic crystal of Curdlan shows four triple helices associating via O(4) and O(6) hydrogen bonding to produce longer-range order (Fig 4). The unit cell would be drawn as a parallelogram from the centre of each of the four helices, showing the presence of six glucose residues in the unit cell. It is of interest to note that the hydroxymethyl groups on C(6) decorate the outside of the triple helices, not affecting internal structure but being critical for longer-range order. For applications then, functionalization at the C(6) position would be inconsequential to the triple helices themselves but may change the overall crystallinity and gelation profile[27].

Investigation of hydrated Curdlan in comparison to the dehydrated form began in 1983. The crystalline arrangements were similar between the two forms except for the dimensions of the unit cell showing an increased fiber repeat parameter, indicating a loss of symmetry and an increase in the volume of the unit cells in the hydrated state. The increased volume was suggestive of the incorporation of significant amounts of water into the triple helix. Approximately 18 to 36 molecules of water were found per unit cell that all contributed significantly to the hydrogen bonding of the helical structures[28].

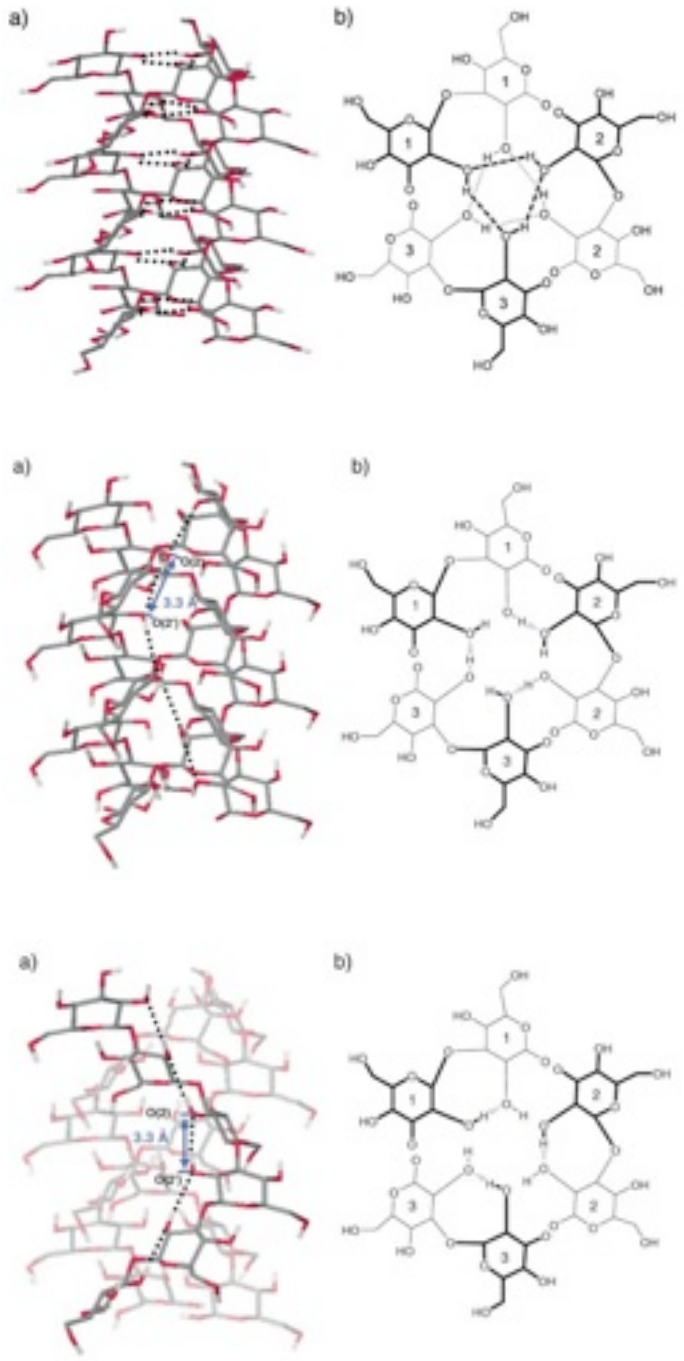

Figure 3. Hydrogen Bonding Schemes for the Curdlan Triple Helix[44]. (Top) Original Right-Handed Triple Helix with Inter-Strand H-Bonding, **(Middle)** Left-Handed Triple Helix with Inter-Strand Bonding, and **(Bottom)** Right-Handed Triple Helix with Intra-Strand H-Bonding, (a) Model of Triple Helical Formation, (b) X-Y Projection of helical strands.

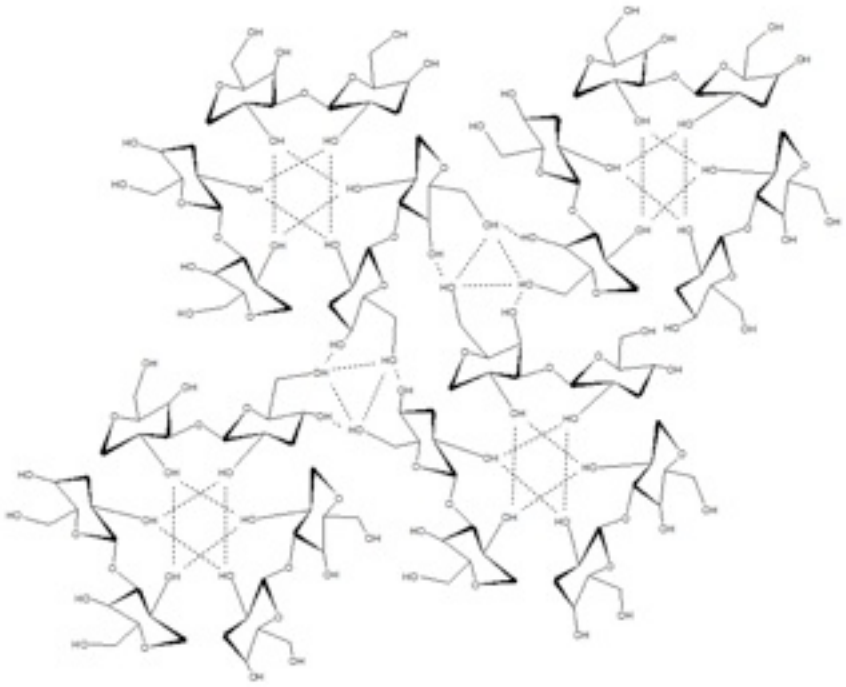

Figure 4. Periodicity in Highly Crystalline Curdlan. Four triple helices held by hydrogen bonding between O(4) and O(6) oxygens,

Although these studies are generally considered conclusive as to the crystallographic forms of Curdlan, there still exists some controversy. The presence of two additional hydrogen bonding schemes have been postulated. Besides the originally proposed inter-strand hydrogen bonding (Fig 3; top), the association of single helices without inter-strand hydrogen bonding, instead relying on Van der Waals forces to maintain the triple helix, has been found to be favorable via simulation based on an improvement in the linearity of the H-bond, despite an unfavorable increase in bond length (Fig 3; bottom). A third H-bonding scheme that maintains inter-strand bonding to hold the triple helix together but requires O(2) H-bonds with adjacent atoms has also been proposed, ultimately requiring a left-handed helix instead of the traditional

right-handed helix (Fig 3; middle). Considering heat of formation and bond energy, the new hydrogen bonding structures were thermodynamically favored in simulation[44]. The existence of these new hydrogen bonding structures have not yet been verified experimentally but they offer insight into the transition of bonds that may occur during crystallization as single helices aggregate and rearrange hydrogen bonds to form triple helices.

2.1.2 Current Understanding of Curdlan Gelation

Curdlan gels have been studied since 1967 wherein gelation was observed above 55 °C when heated from aqueous or dilute alkaline solutions[40]. Curdlan gels may be obtained by simply hydrating Curdlan under heating or by neutralization from alkali solution[41]. The general methods for the gelation of Curdlan follow (Table 1).

Table 1. Methods of Curdlan Gelation

Type	Crystallinity	Method
Native	< 30%	N/A
Curdlan Hydrate	High	55-145 °C in Humidity or from Suspension Neutralization of Alkaline Solution
Dry Curdlan	Very High	Dry Curdlan Hydrate

Gelation is normally carried out from 10% (w/v) suspensions in water, dilute alkaline solution, buffer[45] or with 10% solutions in DMSO that are extruded into methanol and dried before heating under humidity[27]. Gelation can be separated into two distinct regimes. Treatment between 55-80 °C induces the formation of a low-set gel. Low-set gels may dissociate upon cooling but they may be further treated to strengthen the gel into the next regime. Treatment between 80-145 °C induces the formation of a thermally irreversible high-set gel that will not melt and cannot be further crystallized once cooled[45]. Gelation is also possible by neutralizing a 0.1 M NaOH solution of Curdlan with 0.1 M HCl and purifying the gel suspension by dialysis[46]. Dissolution of crystalline Curdlan may be carried out using DMSO, a good solvent for Curdlan that disrupts hydrogen bonds or by increasing alkaline concentration[47, 48]. The gelation mechanism of Curdlan has been heavily investigated in the literature (Table 2).

Table 2. Characterization Techniques for Curdlan Gelation

Method	Parameter(s)	Reference
Nuclear Magnetic Resonance	^{13}C Peak Intensity and Width	43
Electron Microscopy	Direct Observation	46
Differential Scanning Calorimetry	Enthalpy Change	49
Attenuated Total Reflection Infrared Spectroscopy	Infrared Band Shifts	45
Rheology	Storage Modulus	41
Nuclear Magnetic Resonance Relaxometry	Chain Mobility	41
Atomic Force Microscopy	Direct Observation	50
Single Molecule Force Spectrsoscopy	Interaction Forces	51

^{13}C Nuclear Magnetic Resonance (NMR) has been used to observe the proportions of single to triple helices in Curdlan gels formed from aqueous and dilute alkaline suspensions. Significant line broadening for the six carbon peaks between 60-100 ppm occurred due to the lack of chain mobility in the triple helical structures (Fig 5; Left) with these peaks sharpening slightly as the alkaline concentration was increased and then drastically sharpening around 0.22 M NaOH, indicative of the formation of random coils (Fig 5; Right). This behavior is consistent with studies on the loss of crystallinity in alkaline solutions[48]. Downfield peak shifts of C(1), C(3), and C(4) during gelation verified the formation of an ordered helical structure as these shifts were ascribed to a restriction in rotational motion of the glycosydic linkage and the development of hydrogen bonding between helices. Since it was reasoned that the entirety of the ^{13}C signal was due to single helical structures due to the immobilization of chains in multiple-

helical networks it was concluded that Curdlan gels might contain more significant populations of single helices[43].

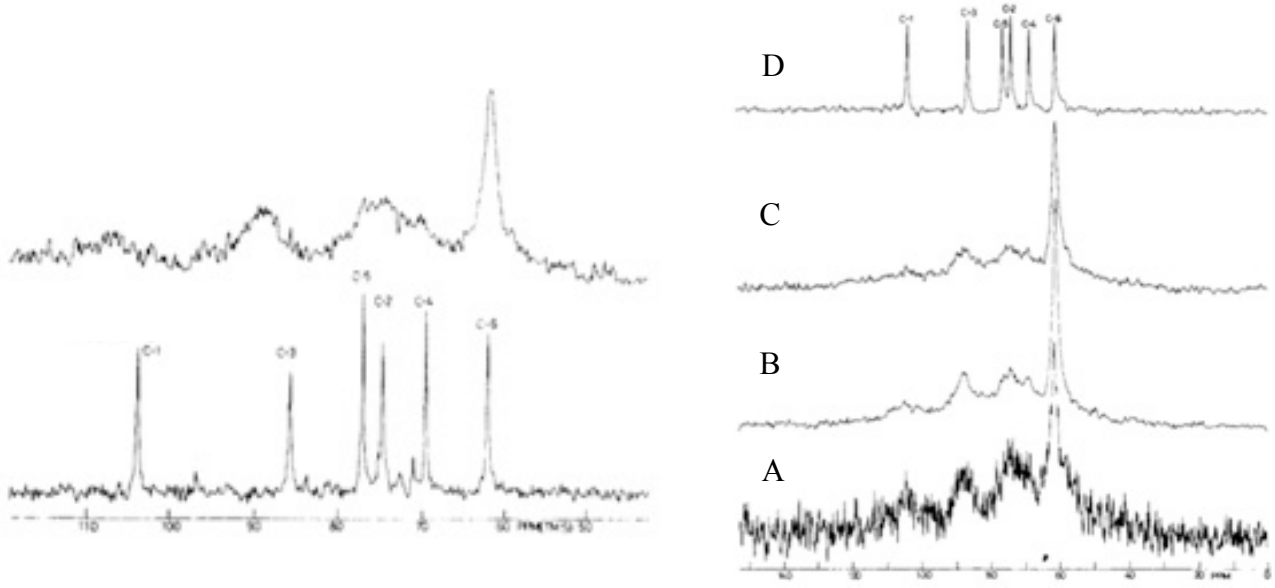

Figure 5. NMR Peak Broadening and Effect of Alkaline Concentration[43]. The six ^{13}C-NMR Peaks of Curdlan show significant broadening when moving from Native Curdlan **(Left: Bottom)** to the Resilient Gel **(Left: Top)** and the peaks sharpen when exposed to increasing concentrations of NaOH solution **(Right)**: (A) Aqueous Suspension, (B) 0.06 M, (C) 0.19 M, and (D) 0.22 M.

Electron Microscopy (EM) has been used to obtain images of the gelling behavior of Curdlan. SEM images revealed 30 Å fibrils in 100-200 Å bundles with micrographs clearly showing the similarity in helical conformations formed by heating to low-set gels and neutralization, both forming rope like Curdlan fibers (Fig 6A,B). Images of samples heated to 90 °C after heating at 60 °C (Fig 6C) demonstrated that low-set gels may be further crystallized to high-set gels. Re-heating at higher temperatures (120 °C) resulted in a return to the less ordered structure (Fig 6D). The formation of the low-set gel was proposed to be primarily composed of

hydrogen bonds that initially break when heated to release microfibrils and then reorganize to rebuild greater crystallinity. High-set gels were believed to gain additional strength from hydrophobic interactions[46].

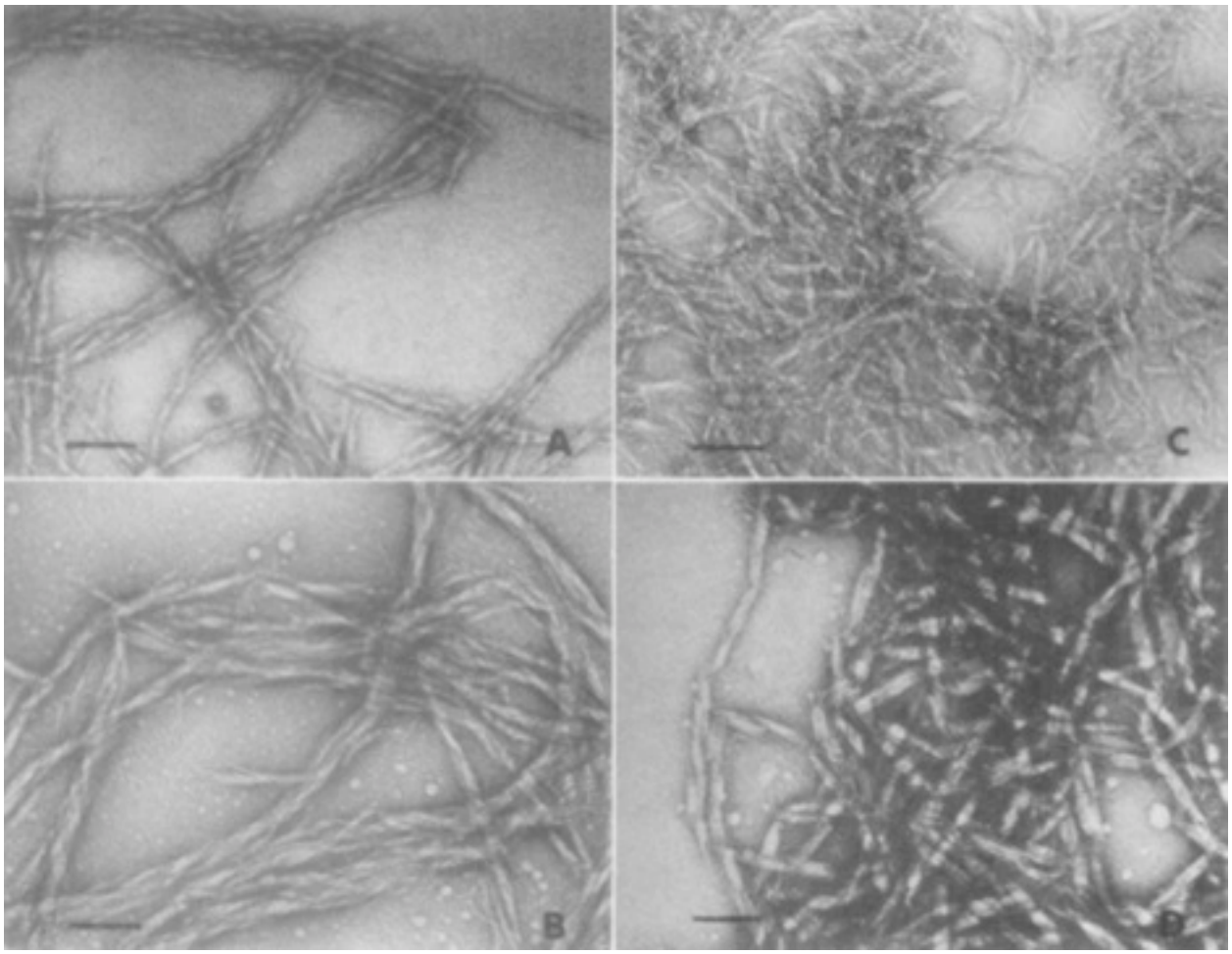

Figure 6. Electron Micrographs of Curdlan Gels[46]. (A) Curdlan gelled by Neutralization shows 100-200 angstrom bundles with **(B)** Heating to low-set gel at 60 °C improving crystallinity, **(C)** Re-heating at 90 °C showing further increases into the high-set regime, and **(D)** Re-heating at 120 °C showing a decrease in crystallinity.

Differential Scanning Calorimetry (DSC) demonstrated the temperature-induced gelation of Curdlan in an aqueous suspension. Endothermic swelling was observed at 56 °C, highest

crystallization at 142 °C, and melting of the gel at 154 °C (Fig 7). Thus, low-set, thermally reversible gels that may be further crystallized are created in the temperature range of 60-80 °C, containing small amounts of triple helices and high-set, thermally irreversible gels are created at temperatures up to 150 °C with much higher crystallinity[49].

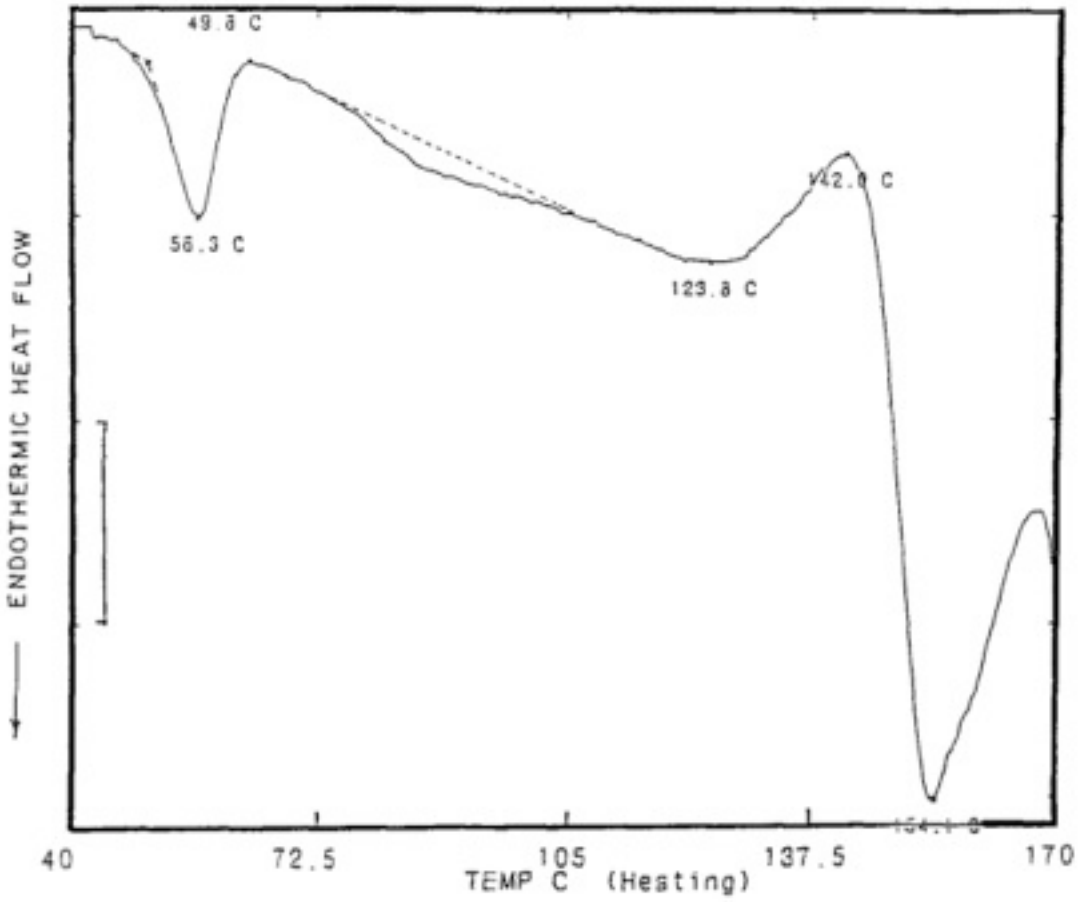

Figure 7. Differential Scanning Calorimetry Study of Curdlan[49]. DSC of a 4% aqueous suspension reveals an initial endothermic event at 56 °C as Curdlan is heated to a low-set gel and another event at 142 °C when Curdlan reaches its highest point of crystallinity before melting.

Attenuated Total Reflectance Infrared Spectroscopy (ATR-IR) allowed observation of reversible band shifts assigned to the formation of hydrogen bond networks with water that were observed after only 5 minutes at 30 °C. Under heating, the band at 1110 cm^{-1} shifted at 55.9 °C,

verifying the DSC characterization gelation scheme. High-set gels were produced at 95 °C with less than 10% reversibility possible as monitored by the ratio of the peaks at 1080 and 1045 cm^{-1} with low-set gels showing much more reversibility[45].

Rheological studies measuring the storage modulus of Curdlan gels throughout the gelling temperature range demonstrated that there is an initial increase in storage modulus before the low-set gel temperature as single helices aggregate followed by a decrease as these helices break hydrogen bonds and then a gradual increase as the helices re-organize to form more crystalline triple helical structures[41]. This result confirms the initial breaking of bonds observed in the formation of the low-set gel[46].

NMR Relaxometry studies further confirm this result by measuring chain mobility during temperature ramping, showing a characteristic decrease in chain mobility as the single helices aggregate, followed by an increase as they melt, and a decrease as triple helix crystals are formed. It was also demonstrated was that holding temperature in the gelation regime initiated an annealing of triple helix crystals with the implication that discrete low-set and high-set gels are perhaps a misleading terminology as a continuum of states exists[41].

AFM studies have been carried out on both Curdlan and branched 1,3-β-glucans, allowing the observation of fiber dimensions[50, 52]. Three nanometer thick fibers were observed for Curdlan that formed network structures of fibers on mica from 0.01 M NaOH suspensions (Fig 8: Left). Variation of the height confirmed the heterogeneity of Curdlan at this lower alkaline concentration. Higher concentrations of alkali (1 M NaOH) demonstrated the thickness of fibers falling to 0.5 nm in some places but the network structure was still intact in places, suggesting incomplete solubility even at high concentrations of NaOH (Fig 8; Left). The observation of network structures even at high alkaline concentrations suggested that the thermal

gelation mechanism involved partial breaking off of random coils from parent fibers that form triple helices to cross-link the parent fibers (Fig 8; Middle, Right). The previously observed increase in hydrogen bonding followed by bond breakage before triple helix assembly suggests that collapsed random coils might form intramolecular hydrogen bonds to single helices that then associate with other single helices, break intra-structural hydrogen bonds, and then reform inter-strand hydrogen bonds to create triple helical structures. Hydrophobic interactions then also play a key role in holding the triple helices together [50].

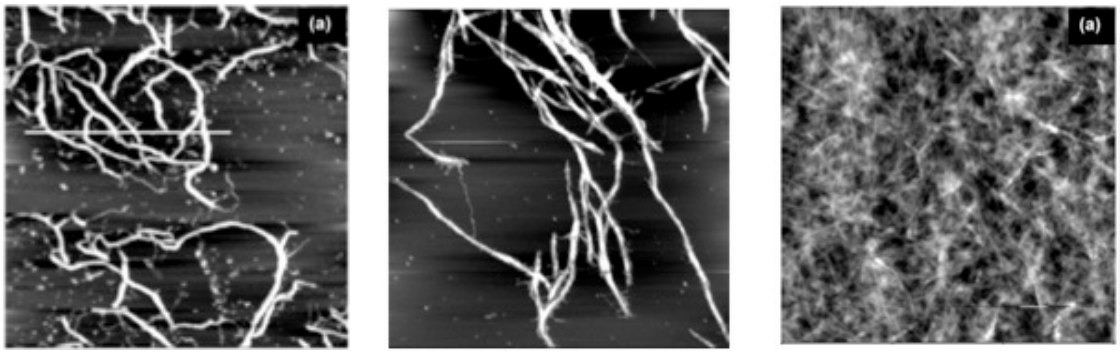

Figure 8. Atomic Force Microscopy Scans of Curdlan Gelation[50]. (Left) Residual network structure in 1M NaOH solution. **(Middle)** 0.1 M NaOH suspension of Curdlan that was heated at 90 °C for 4 hours. **(Right)** Bulk-gel precursor from the same suspension demonstrating the formation of densely cross-linked networks.

Curdlan has been investigated with Single Molecule Force Spectroscopy (SMFS) to elucidate the transitions that occur during increased concentrations of sodium hydroxide. Experimentation on 0.5 M NaOH solutions of Curdlan demonstrated the stretching of single Curdlan chains, indicative of random coils of Curdlan in alkaline solutions of this concentration. A helix-coil transition was observed in 0.1 M NaOH with a 60 pN force proposed to be required to begin the unwinding of triple helical structures. At 0.2 M NaOH, it was believed that the observed phenomenon was the unwinding of single helices from duplex structures, as the unwinding force was only 40 pN. This transition from triple helices to single helices and then random coils from 0.19-0.24 M NaOH agreed well with prior predictions and elucidated a possible intermediate duplex state between triple helix and random coil that may be involved in gelation[51].

Despite the extent of characterization efforts, the exact mechanism for gel formation of Curdlan is disputed. Some harmony is materializing out of the use of more visual techniques such as AFM, explaining some of the otherwise strange bond breakages and formations observed via rheology and NMR studies. Despite this, AFM studies have introduced confusion of their own by showing the presence of random coil networks even at very high alkaline concentrations. The possible mechanism of cross-linking of these fibers by the increasing populations of single and triple helices to create Curdlan gels is a promising lead. It is the prevalence of complex mixtures of random coils, single helices, and triple helices at different alkaline concentrations and temperatures that have made the elucidation of the mechanism of Curdlan gelation a moving target as characterization techniques improve to gain a better understanding of these populations.

2.2 Bioactivity of 1,3-β-glucans

The interaction of 1,3-β-glucans with immune cells generates a potent pro-inflammatory effect consisting of stimulation of the production of cytokines, increased phagocyte and lymphocyte proliferation, oxidative burst, and phagocytosis against opsonized tissues. This pro-inflammatory effect has led to a number of therapeutic applications using 1,3-β-glucans to impart tumor inhibition, disease resistance, and wound healing. These processes are caused by a number of different initiating pathways.

2.2.1 Activation of Alternative Complement Pathway

Zymosan, a fraction of sterilized cell wall from *Saccharomyces cerevisiae* containing 70% β-glucans, was known to be an initiator of the alternative complement pathway since the discovery of the properdin pathway in 1954, forming an active complex with properdin that allowed the consumption of C3b, complement cascade, and the destruction of the pathogen[53]. Interaction with C3b initiates the formation of membrane attack complex (MAC) and the generation of opsonins among many other processes. Kinetic studies on the formation of zymosan-properdin complexes were carried out and the involvement of factor B in the process of C3 and C5 consumption was demonstrated[54]. Later, it was verified that there neutral 1,3-β-glucans could yield a prominent activation of the alternative complement pathway, ruling out the hypothesis that zymosan activation occurred due to the presence of phosphate groups in the unpurified fraction[55].

2.2.2 Interaction of 1,3-β-glucans with Phagocytes and Lymphocytes

The antitumor activity of zymosan was originally believed to be due to a lipid fraction until it was demonstrated that isolated polysaccharide fractions of zymosan decreased the half-

life of colloidal carbon 10 times when administered to mice by generating hyperplasia and hyperfunction in immune cells[56]. The cellular membrane receptor on phagocytic macrophages for the binding of 1,3-β-glucans was the focus of a large volume of research with the candidates being a complement receptor or Dectin-1, both of which were found to be dependent on iC3b opsonization, the proteolytically deactivated form of the complement protein C3b. It was demonstrated in 1986 that Complement Receptor 3 (CR3) was responsible for the binding of opsonized zymosan[57]. In 1996, it was demonstrated that macrophages bearing CR3 were capable of attacking any iC3b-opsonized pathogen in the presence of 1,3-β-glucans[58]. The complement protein C3b normally coats pathogens marking them for detection by Complement Receptor 1 (CR1) or activation of complement cascade. The deactivation of C3b to iC3b is a regulatory mechanism to avoid unnecessary immune activity. Since iC3b is recognized by CR3 in the presence of 1,3-β-glucans, CR3 and the iC3b opsonin play a critical role in innate immunity towards fungal and microbial pathogens, mediated by the presence of 1,3-β-glucans in these pathogens. Independently delivered 1,3-β-glucan could then yield a targeting of cancer cells with surface coatings of iC3b[58].

Using murine models, the role of CR3 and Dectin-1 were compared for the binding of unopsonized zymosan. It was demonstrated using fluorescent labeling that CR3 deficiency was inconsequential in murine models[59]. Further evidence for this result was provided in 2003 where the production of a cytokine, Tumor Necrosis Factor Alpha (TNF-α), was used as a measure of receptor efficacy when macrophages were retrovirally transduced to produce large amounts Dectin-1. The transduced macrophages bound more unopsonized zymosan and showed a dose dependent secretion of TNF-α[60].

In the most recent studies with human neutrophils, no phagocytosis of unopsonized zymosan was observed when CR3 was blocked, no zymosan binding was possible in CR3 deficient humans, and the efficacy of respiratory burst was inconsequential with Dectin-1 primed zymosan compared to plain zymosan. It was concluded that although Dectin-1 plays an essential role in mediating the interaction of 1,3-β-glucans with immune cells in murine models, functional CR3 was required for the efficient binding and response to both opsonized and unopsonized zymosan in humans[61]. Figure 9 shows two critical elements to the structure of CR3, the β-Chain that interacts with a 1,3-β-glucan and the α-Chain that interacts with an iC3b opsonin. The binding of 1,3-β-glucans to the β-chain initiates cell stimulation as well as a conformational shift in the α-Chain that allows CR3 to bind iC3b-opsonized pathogens (Fig 10)[62].

Although most studies focus on the binding of 1,3-β-glucans to CR3 or Dectin-1 on phagocytes, the primary form of activity of many 1,3-β-glucans such as lentinan is interaction with and stimulation of T-cell and natural killer cell activity to promote acquired immune response and lysis by other means such as the release of perforins and granzymes. Lentinan also interacts with T-cells and natural killer cells to promote proliferation of the cells themselves or proliferation with desirable IL-2 cytokine receptors[63, 64]. Very recently, increases in lymphocyte proliferation were observed as a result of all 1,3-β-glucan treatments with Curdlan at concentrations up to 800 ug/mL yielding the greatest effect[65]. Thus more research into the effects of 1,3-β-glucans on lymphocyte populations is necessary to expand the current understanding of pharmacological effects.

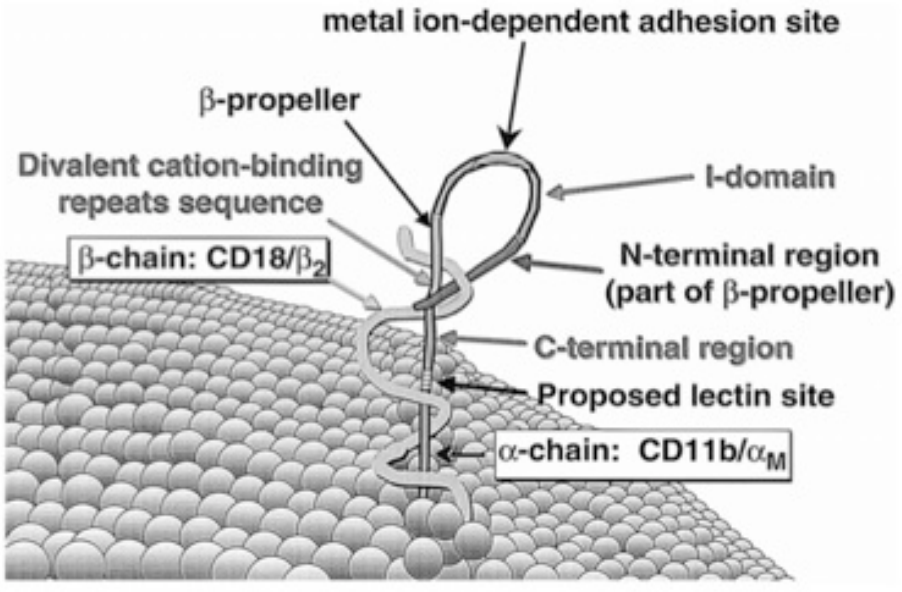

Figure 9. Schematic of the Domains of Complement Receptor 3[62]**.** Complement Receptor 3 consists of the β-chain which interacts with 1,3-β-glucans and the α chain that experiences a conformation shift, allowing the recognition of iC3b opsonins.

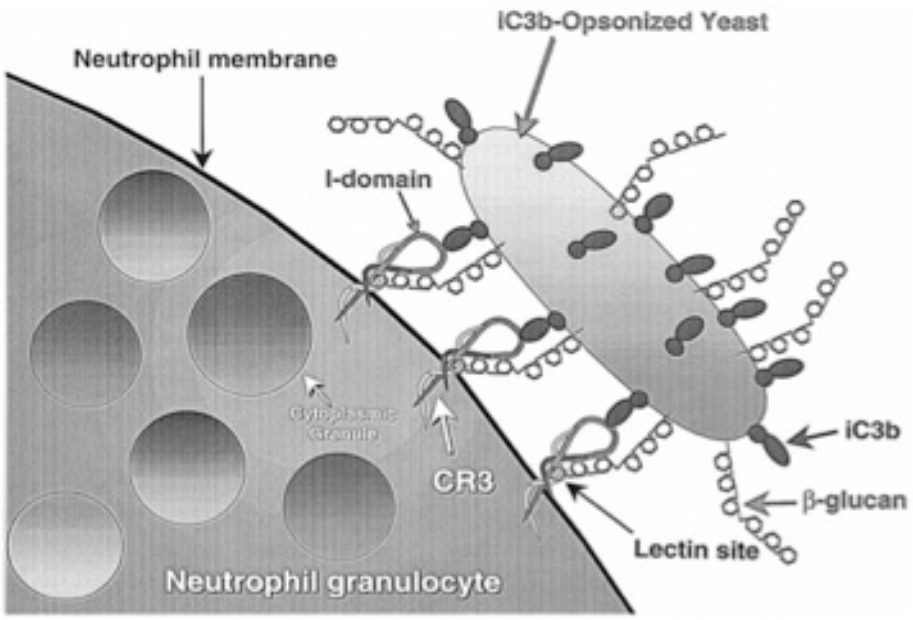

Figure 10. β-Glucans Initiate a Conformational Shift to Allow Response to iC3b Opsonin[62]**.** Under normal circumstances, CR3 dual interactions with 1,3-β-glucans and iC3b allow for the recognition of fungal pathogens but this system has been leveraged for cancer therapy.

2.2.3 Pharmacological Effects of 1,3-β-glucans

1,3-β-glucans stimulate the production or induction of a variety of pro-inflammatory mediators and cytokines including TNF-α**,** Interferon- γ (IFN-γ), Granulocyte-Macrophage Colony Stimulating Factor (GM-CSF)[66], Inducible Nitric Oxide Synthase (iNOS), Macrophage Inflammatory Protein 2 (MIP-2), and a host of Interleukins (IL-1Iβ, L-8, IL-10, IL-12, IL-4, IL6)[65]. This stimulation was demonstrated to occur at the mRNA level with MIP-2 and TNF-α similar to lipopolysaccharide (LPS) stimulation[67, 68]. The production of these pro-inflammatory mediators is linked to activation of Nuclear Factor- κB (NF- κB). A recent study has highlighted the critical role of a phospholipase C enzyme and a Calcium ion flux in the intracellular signaling resulting from receptor activation[69].

Oxidative burst is an innate immune response to pathogens external to or internalized by phagocytes that is characterized by the release of reactive oxygen species (ROS). Different types of ROS include peroxides and peroxynitrites formed from superoxide anions and nitric oxide that are responsible for peroxidation of lipids and proteins and the cytotoxicity of microbes. Curdlan was shown to effectively mediate the induction of iNOS and production of nitric oxide *in vitro* in rat macrophages[67]. Very recently, a variety of 1,3-β-glucans were shown to stimulate the production of ROS in differing amounts dependent on branching and chain length[65].

Phagocytosis of pathogens or opsonized pathogens in response to 1,3-β-glucan stimulation has been studied much less than the corresponding oxidative burst and cytokine producing pharmacological effects in the recent literature. However, good theories exist as to the mechanism of this behavior[62]. An *in vitro* phagocytosis test using synthetic microbeads was recently formulated, serving as an excellent starting point for the comparison of different 1,3-β-glucan structures[70]. Elimination of pathogens or cancer cells can also occurs by acquired cellular

immune pathways involving cytotoxic T-cells or natural killer cells as was initially demonstrated with lentinan[63] and later demonstrated with most 1,3-β-glucans[65].

The pharmacological effects of 1,3-β-glucans are heavily dependent on the specific conformation and structure of the polysaccharide. When studying macrophage activation by 1,3-β-glucans *in vitro*, macrophage activation was observed with the addition of 10-100 ug/mL and enhanced by pre-treatment with sodium hydroxide, dimethylsulfoxide, or zymolase to release free glucans from the particulate systems. Since treatment with sodium hydroxide or dimethylsulfoxide causes the production or single helices and random coils from more crystalline arrangements, it was concluded that the single helix was the most potent conformation for macrophage activation. In addition, longer 1,3-β-glucans were found to be necessary as shorter laminaroligosaccharides showed much less activity[68]. These findings were consistent with early results suggesting that the single helix was critical[43, 71] and that shorter 1,3-β-glucans could not produce iC3b recognition in CR3[58]. In the most recent studies, these effects along with the effects of branching continue to be investigated[72]. Despite the fact that the removal of branching was the only way to generate an immunomodulatory response from pachyman[18], other studies suggest that a complex branching structure in fungal 1,3-β-glucans may be more effective[20]. No firm conclusion yet exists in the literature pointing to the most potent conformation and structure of a 1,3-β-glucan for therapeutic usage but it is generally accepted that the single helix is critical and higher molecular weight polysaccharides are superior.

2.3 Pharmacological Applications of 1,3-β-glucans

2.3.1 Cancer Inhibition

In combination with radiotherapy and/or chemotherapy, the 1,3-β-glucan, lentinan, has been used for cancer immunotherapy in Japan since 1986 for the treatment of lung, gastric, and cervical cancers[31]. In the early studies on lentinan with subcutaneous implantation of sarcoma 180 into mice, intraperitoneal injection of 1-4 mg/kg of lentinan over 10 days yielded a tumor inhibition of 99.6% and inhibition ratios of 96% were also found with pachymaran, the synthetically de-branched form of pacyhman[18]. A number of theories on the nature of the antitumor effects have arisen in the literature. The effects of lentinan and pachymaran are thought to rely heavily on T-lymphocytes as the removal of the thymus or treatment of mice with antilymphocyte serum (ALS) virtually eliminated antitumor effects[63]. This was verified in 1992 when lentinan was found to increase natural killer cell activity and the proliferation of T-cells with IL-2 receptors[64]. Experiments with bovine serum albumin (BSA) showed that denaturation of protein helices could be linked to the antitumor mechanism of lentinan as only those polysaccharides that denatured the protein showed antitumor activity[73]. The generation of new serum proteins was also thought to be linked to the T-cell mediated effects of lentinan[74]. 1,3-β-glucan derivatives such as pachyman, pachymaran, and corresponding derivatives have been found to activate the alternative pathway of complement, involving factor B, as opposed to the T-cell mediated route[55].

Throughout the literature, other 1,3-β-glucans showing similar effects against solid sarcoma 180 were discovered. In the early studies in the 1970's, scleroglucan was found to produce inhibition ratios of 90.4% at a dose of 2.5 mg/kg and Curdlan was found to inhibit tumors from 99-100% with doses ranging from 10-20 mg/kg[19]. In 1985, a branched 1,3-β-glucan,

grifolan, was found to inhibit solid sarcoma 180 up to 97.9% [75]. In 2001, a complex branched 1,3-β-glucan from *Agaricus Blazei* was found to inhibit up to 99.3% of tumor growth[20]. The robust antitumor effects of various 1,3-β-glucans have lead to the modern use of 1,3-β-glucans as adjuvants to monoclonal antibody treatments. Human tumor xenografts from melanoma, epidermoid carcinoma, breast carcinoma, metastatic lymphoma, and daudi lymphoma were affected positively by combination treatments of 1,3-β-glucans and antibodies yielding tumor inhibition and survival rates greater than individual treatments[76]. A recent review considers the topic of combined treatments for cancer immunotherapy in more detail[32].

To improve the usability of 1,3-β-glucans, a significant amount of work has gone into the development of water-soluble derivatives that retain antitumor efficacy. Early work with the development of water-soluble carboxymethylpachymaran showed tumor inhibition ratios up to 99.6% in solid sarcoma 180 with doses of 5 mg/kg, equal with lentinan. Interestingly, the use of the water-soluble derivative allowed for the use of other injection routes besides intraperitoneal injection to obtain the same result[77]. Other 1,3-β-glucans including hydroxymethylpachyman and hydroxypropylpachyman showed up to 100% inhibition at 5 mg/kg in solid sarcoma 180[77]. In 1979, various water-soluble carboxymethylglucans were synthesized that also showed high antitumor activity[78]. Carboxymethyl Curdlan in particular is used extensively in modern applications. Water-soluble glucosyl, sulfoethylated, and sulfopropylated Curdlan derivatives also retain antitumor activity[79, 80]. All of these results suggest that solubility of the 1,3-β-glucan is not a critical factor for antitumor activity.

2.3.2 Infection Resistance

Since 1,3-β-glucans cause cytokine production, oxidative burst, immune cell proliferation, and increases in phagocyte and lymphocyte activity, 1,3-β-glucans have been

investigated for use in increasing overall host immunocompetency. In 1978, It was demonstrated that mouse survival rates for immune challenge with staphylococcal infection increased dramatically with 3% mortality observed in 1,3-β-glucan treated mice vs. 30% in the control group[81]. More recently, oral administration of 1,3-β-glucans to promote resistance to fungal and bacterial infection has been attempted with a full pharmacokinetic characterization. It was demonstrated that the administration of glucan phosphate, laminarin, and scleroglucan through oral ingestion may be advantageous for obtaining a sustained absorption from the gastrointestinal tract, that hepatic clearance of 1,3-β-glucans was ineffective, and that different 1,3-β-glucans had different absorption profiles with laminarin and scleroglucan showing biphasic plasma absorption. Oral administration led to the secretion of interleukins, an increased expression of Dectin-1 on macrophages, and an increased expression of Toll-Like Receptor 2 on dendritic cells. As a result, survival rate for *Staphylococcus aureus* bacterial and *Candida albicans* fungal challenge increased 50% in mice through oral administration[22].

This ability to impart infection resistance has been of growing interest with a growing volume of work attempting to increase immunocompetency in fish and pigs. In 1991, Curdlan, inulin, krestin, laminarin, lentinan, schizophyllan, scleroglucan, yeast glucan, and zymosan were tested to investigate an improvement in bacterial resistance for *Cyprinus Carpio L.* Carp against *Edwardsiella tarda* bacteria. At a dose of 10 mg/kg, schizophyllan had a 60-80% survival rate and lentinan and scleroglucan had 55-75% survival rate on day three vs. complete mortality in control groups. When challenged with *Aeromonas. hydrophila,* survival rate was 70% for lentinan, 80% for scleroglucan, and 60% for schizophyllan when treated with 5 mg/kg after 5 days vs. complete mortality in control groups[21]. A later study found similar results with tilapia and grass carp towards infection with *Aeromonas Hydrophila*[82]. Resistance to infection with

Streptococcus suis bacteria in weaning pigs was negative in 1995[83] but more recently, increased levels of TNF-α were observed in weaning pigs and an interesting synergistic effect with vitamin C supplements was postulated[84]. In addition, a positive resistance to LPS challenge was observed[85]. The most recent *in vivo* studies showed a resistance to intestinal colonization by Enterotoxigenic *Escherichia coli* (ETEC), fewer bacteria in faeces, and less severe diarrhea[86]. Recent *in vitro* studies confirm the stimulating capacity of a variety of 1,3-β-glucans, demonstrating that porcine leukocytes show increased cytokine and ROS production and increased proliferation in response to 1,3-β-glucans[65]. It is now clear that the differences in results obtained over >20 years of research into improving resistance to infection in various species are highly dependent on the specific 1,3-β-glucans used, their concentration, and their conformation during administration.

2.3.3 Viral Resistance

Similar to work in resistance to bacterial and fungal challenge, sulfated 1,3-β-glucans have been tested for the ability to impart resistance to viral infection to malaria, herpes simplex virus (HSV) [87, 88], and HIV. In early studies, Curdlan sulfate completely inhibited HIV virus infection in MT-4 cells at 3.3 ug/mL as characterized by the lack of virus specific antigens[89]. These results were consistently verified[90-92], leading to ongoing clinical trials. Malaria infection was resisted in the presence of Curdlan sulfate *in vitro* through an inhibited fusion mechanism[87]. More recently, sulfated 1,3-β-glucans have imparted resistance to infection by HSV through a suggested electrostatic binding to the viral surface that inhibits interaction with host cells[88]. This mechanism of viral interaction was studied with experiments between Curdlan sulfate and polylysine, causing the formation of electrostatic cross-linking to produce clear, strong gels. It was believed that this electrostatic interaction between anionic Curdlan Sulfate and cationic

polylysine may mimic an interaction between Curdlan sulfate and a cationic glycoprotein (gp120) in the viral envelope of HIV, blocking interactions with CD4 receptors[93]. This blocking mechanism has been extensively studied in experiments on HIV inhibition[94-96].

In 1994 it was confirmed that Curdlan sulfate interacts with gp120 on HIV-1 that affects the cell-virus fusion mechanism but that there was no interaction between Curdlan sulfate and CD4 because pretreated cells were vulnerable to infection. This blocking mechanism was supported by evidence suggesting inhibitory action before any viral genetic replication[94, 95]. This result was later confirmed with additional evidence that Curdlan sulfate inhibits TNF-α production that led to T-cell apoptosis caused by gp120 interaction with CD4[92]. An additional mechanism may lie in the mediation of β-chemokines and cytokines by Curdlan sulfate, with demonstrations that MIP-1α, MIP-1β, and MCP-1 were all inhibited whereas RANTES and IL-16, two cytokines known to have anti-HIV activity, were enhanced[97].

The synthesis of Curdlan sulfates in varying conformations and their incorporation into other systems have received attention as well[98]. Azidothymidine (AZT), a nucleoside analogue that inhibits viral reverse transcriptase has been chemically bonded to Curdlan sulfate with the hope of using the tendency of Curdlan sulfate to concentrate in the lymph nodes and bone marrow to deliver drugs to the RES, using Curdlan sulfate as an HIV inhibitor and drug delivery vehicle. A hydrophobic alkylene group was used a spacer between the two components that would be susceptible to enzymatic hydrolysis. The overall drug delivery system demonstrated the enzymatically-triggered release of AZT[89, 99]. An additional opportunity follows the recent research around fullerene derivatives as anti-HIV agents[100]. Water-soluble Curdlan Sulfate-C_{60} conjugates have been synthesized that combine the anti-HIV activity of Curdlan sulfate and fullerenes[101]. Alongside new conjugates and delivery vehicles, research is also working on

improving the synthesis of Curdlan sulfates. A growing amount of work exists on the development of easy functionalization mechanisms by 'Click Chemistry' [102-104]. Some of the most recent work has investigated the use of ultransonication for sulfation of Curdlan with impressive results showing four-fold increases in the degree of substitution. However, molecular weights were decreased significantly[105].

2.3.4 Wound Healing

Wound healing effects of 1,3-β-glucans have been studied extensively as a growing application. Suggested effects of 1,3-β-glucans related to wound healing are improved transport of macrophages to the wound site[106] and improved collagen deposition[24]. The effect on collagen deposition was originally thought to be indirect through the stimulated release of growth factors from macrophages but a recent study has shown that insoluble glucan from zymosan, laminarin, and glucan phosphate can interact, sometimes only partially, with Normal Human Dermal Fibroblasts (NHDF). This binding stimulated NF- κB activity and IL-6 mRNA expression[107]. The discovery of increases in NF- κB activity and direct binding to NHDF's has stimulated investigation into the ability of 1,3-β-glucans to induce collagen synthesis. Type I and III collagen biosynthesis was substantially improved with treatment with 1,3-β-glucans in recent studies by measurement of pro-collagen mRNA and hydroxyproline levels[96]. Consistent with these findings, Beta-glucan Collagen Matrix (BGC) was evaluated in the treatment of pediatric burns with observed reduction in pain and required analgesic, reduction in the necessary number of wound dressing changes, and improvements in healing and cosmetic appearance[108].

2.4 Structural Applications of 1,3-β-glucans

The ability of 1,3-β-glucans to form helical structures that can be gelled with the application of heat and humidity has generated a fast growing volume of research on the use of these polysaccharides as structural agents to provide scaffolding for the formation of macroscopic and nanoscale structures.

2.4.1 Food Gels

The gelation mechanism of Curdlan has been heavily utilized in food science after the U.S Food and Drug Administration (FDA) approved Curdlan for addition to food in 1996[29, 30]. Curdlan gels have been used in improving food stability through freezing and thawing cycles[29, 109], reducing fat content in deep-fat frying applications[30, 110], creating fat mimetic systems[111, 112], and encapsulation and release of pH sensitive pigments[113].

Nakao investigated the gel strength and syneresis of Curdlan gels at room temperature and when frozen and formed into strawberry and honey flavored gels, soy milk noodle-like gels, and mixtures with other gelling agents. Gels were subjected to thermo-irreversible gelling temperatures of 100-130 °C and the gel strength was observed to continually increase as heating was applied. Syneresis, as measured by absorbing water from the gel and measuring mass after 20 hours of refrigeration, increased with gelling temperature and decreased with concentration. Freezing and thawing increased syneresis but Curdlan gels had higher gel strength after thawing than carrageenan, agar-agar, and konjac. The addition of waxy corn starch and sucrose reduced syneresis. The creation of thin-layered Curdlan gels containing various flavoring agents to replace condiments and tofu noodles stabilized with Curdlan rather than coagulation of soy milk with calcium sulfate have been proposed[29]. Combinations of Curdlan, Xanthan, Locust Bean

Gum, and Guar Gum have also been evaluated for freeze-thaw stability with Curdlan and xanthan hydrogel complexes found to be the most stable in terms of viscosity, heat stability, and gel strength[109].

Curdlan has been investigated as an additive to reduce fat content. The ability of Curdlan to act as an oil barrier and repel fat in frying applications and its effects on the physical properties of donuts was investigated. The addition of 1% of Curdlan to the donut batter resulted in a reduction of 5.6% in total fat content and 9% in oil uptake during frying. Curdlan was also found to inhibit moisture loss[30]. This research has also been expanded to the frying of other products, namely akara from cowpea flour (*52*). Curdlan reduced fat content by 10% in akara with mixtures of 1% Curdlan and 20% soybean flour while maintaining texture as long as the composite flour was sufficiently moisturized prior to use[110].

Curdlan has been investigated as a fat substitute in low-fat meat products with 'false-fat' created from a mixture of 3% Curdlan, 10% microcrystalline cellulose, and 1% modified tapioca starch. The 'false-fat' was incorporated into sausages (20%) and compared to sausages made of 20% pork fat. The mixture was comparable to natural pork fat in terms of lubricity, viscosity, mouth feel, and appearance as determined by static viscoelasticity measurements[112]. Curdlan was also added to minced pork as a gelation agent where it was found to form an irreversible gel that retained moisture[111].

The isolation of environmentally sensitive pigments has been an important issue in food science. Curdlan has been used to encapsulate and release pH sensitive blackberry anthocyanins. Spraying of a suspension of ~5% Curdlan and anthocyanin extract into a soybean oil bath and recovering capsules by filtration proved an effective means to stabilize the dye[113].

2.4.2 Environmental Gels

Removal of contaminants from water sources is a critical issue in today's society. Heavy metal removal from water is often carried out with activated carbon particles that contain porous internal structures capable of adsorbing metal contaminants. Application of activated carbon was facilitated by suspending particles in Curdlan gels demonstrating the removal of copper, manganese, lead, and cadmium from oriental herbs with the pore size adjustable based on Curdlan/Carbon ratio[114]. This preliminary research could be extended to water purification.

The removal of Dense Non-Aqueous Phase Liquids (DNAPL) from aquifers was addressed with a Curdlan gel based treatment. Dual columns, one containing coarse sand and the other fine sand were set-up in temperature controllers to simulate temperature fluctuations in Alaskan environments. The two columns were meant to mimic high permeability and low permeability paths of DNAPL during conventional removal techniques. Alkaline solutions (0.01 N NaOH) of Curdlan were added into the coarse sand column, gelling due to the natural acidity of the soil (gelation by neutralization) and restricting flow through the coarse sand column and concentrating DNAPL in the fine sand column. This demonstration of the modification of soil permeability by Curdlan gels was promising for the development of new strategies to remove DNAPL from aquifers[115].

2.4.3 Nanostructure Formation

The helix forming capability of 1,3-β-glucan is attractive for nanoscience applications where structures with dimensions or conformations suitable to interact with single helices are manipulated. The triple helical structures of Curdlan and schizophyllan have been used to encapsulate Single Walled Carbon Nanotubes (SWCNT) that were otherwise insoluble in water. Re-naturing of Curdlan and schizophyllan from a DMSO solution (by addition of water) caused

encapsulation of SWCNTs as observed as helical oblique stripes on the surface of SWCNT bundles through AFM (Fig. 11). This coating was believed to stabilize SWCNTs, avoiding aggregation and improving solubility[116]. Hierarchical superstructures have been assembled using these stabilized one-dimensional carbon nanotubes, utilizing ammonium and sulfite functionalized Curdlan backbones to first encapsulate SWCNT's and then stack the nanotubes into layers via alternating electrostatic interactions [117]. The structures formed may have utility in both SWCNT structure formation and the hierarchical assembly of bio-active polymers such as peptides or nucleotides.

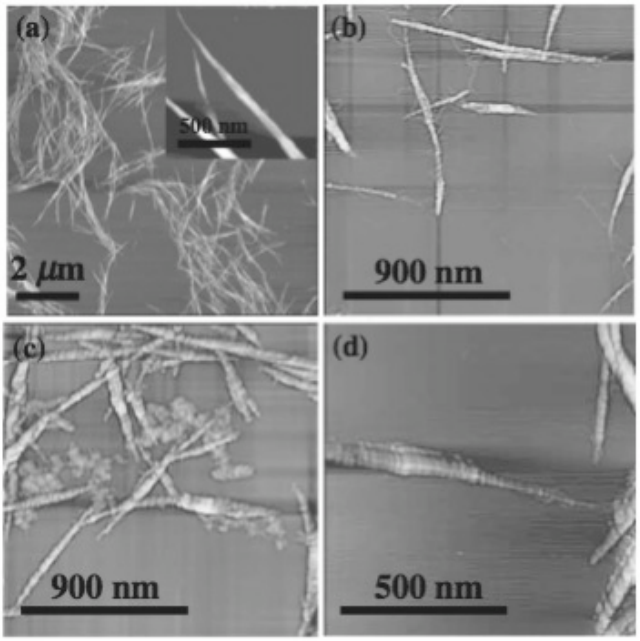

Figure 11. Helical Encapsulation of SWCNT's as seen through AFM[116]**. (A)** SWCNT's, **(B)** Schizophyllan encapsulation, **(C)** Curdlan encapsulation, **(D)** Magnified view of Schizophyllan encapsulation showing helical oblique striations.

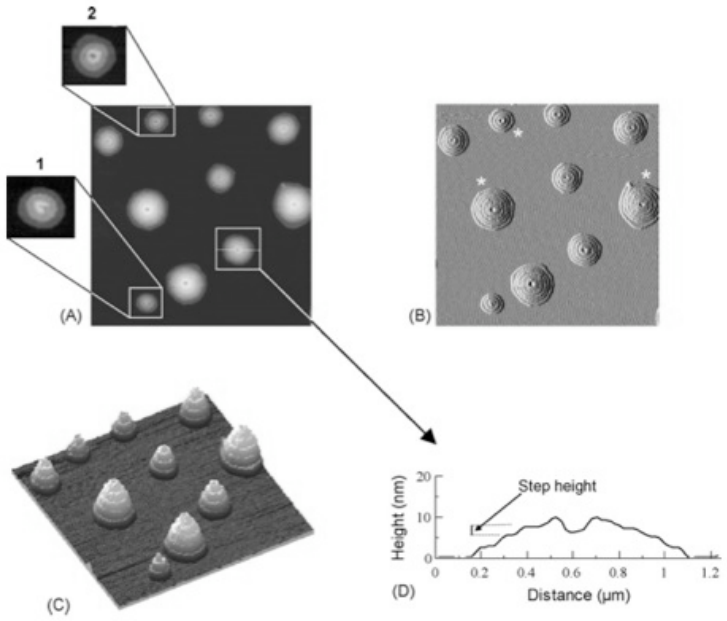

Figure 12. Conical-terraced assemblies of Laminarin as seen through AFM[118]**. (A)** AFM height image, **(B)** AFM amplitude image, **(C)** 3D construction from AFM**, (D)** Cross-sectional height showing the presence of a pore in the center.

The formation of ordered metal nanowires for application in nanoelectronic circuitry has been an ongoing challenge in nanotechnology. Historically these nanowires have been constructed using surfactant assemblies or porous nanostructures to direct growth but recently there has been interest in schizophyllan as a scaffold or templating material for Au nanowires. Mixing Au nanoparticles in water and schizophyllan in DMSO allowed the precipitation of schizophyllan helices containing 1D arrangements of Au nanoparticles. After washing and chemical reduction, photo-induced dissociation, or a combination of both, the helical structure contained ordered arrangements of discontinuous Au nanowires[119]. This finding could be used to create helical micelles containing any sort of nanoparticle including those designed to deliver therapeutic substances, creating functional hierarchical assemblies. The templating effects of schizophyllan have been used in the development of a number of other systems as well including silica[120], oligosilane [36] and porphyrin nanofibers[35], and *in situ* polymerizations[121]. Other 1,3-β-glucan are also currently under investigation for the templating and scaffolding properties including laminarin which has recently been formed into terraced cone-like structures (Fig 12)[118]. These advancements in templating technologies utilizing 1,3-β-glucans provide a more practical and cost effective method to scaffold nanostructures than DNA templating and provide important pharmacological properties in the process.

In addition to nanostructure templating 1,3-β-glucans are currently being used chemically in nanoparticle synthesis. Carboxymethyl Curdlan was used a 'green' biopolymer reducing agent in the synthesis of silver nanoparticles. Light scattering and TEM demonstrated that 40-80 nm particles were formed within 10-15 minutes by reduction of silver ions in CM-Curdlan solution[122].

2.4.4 Liquid Crystals

The ability for 1,3-β-glucans to gel when dialyzed against calcium chloride solution has been utilized to create liquid crystalline gels with interesting refractive index gradients and other optical properties. A stepwise gradient of crystalline order from the outside towards the amorphous center was observed for gelation of a Curdlan alkaline solution against calcium chloride wherein the calcium ions cross-link hydroxyls at the C(6) position. The transition from the random coil conformation in alkaline solution to triple helix in the calcium chloride solution is responsible for this effect as a competition occurs between the states before they cross-link[123]. This system has been studied in terms of the effects of Curdlan molecular weight[124] and used as a model in the liquid crystal gelation of DNA[125, 125]. Using creative experimental setups, these liquid crystalline gels have been developed in the form of polymer beads as well, opening up application in oral drug delivery[126].

2.5 Drug Delivery Applications of 1,3-β-glucans

2.5.1 Drug Impregnated Gels

Gel encapsulation of indomethacin, prednisolone, and salbutamol sulfate in Curdlan gel suppositories has been the hallmark example of Curdlan application in this area. Curdlan suppositories with intended application in rectal administration have been developed wherein Curdlan gels would allow drug diffusion in the lower rectum, avoiding first pass clearance in the liver. The proposed systems an improvement over other suppository systems that immediately dissolve and deliver drug into the colon and consequently the hepatic portal vein. Diffusion controlled release of indomethacin was possible with Curdlan suppositories wherein the release rate was unaffected by hypotonicity or isotonicity[127]. Dry tablet encapsulation of theophylline by

spray drying Curdlan/Theophylline solutions were also demonstrated with good pharmacokinetics[128].

2.5.2 Nanoparticle Drug Delivery

Nanoparticle drug delivery approaches have been successful with the synthesis of solid lipid nanoparticles consisting of cacao butter and Curdlan. Curdlan was believed to coat cacao butter nanoparticles when introduced in an ammonium hydroxide solution. The stabilized nanoparticles were loaded with verapamil, which was quickly released within 12 hours due to its high solubility in the lipid core[129]. Solid lipid nanoparticles consisting of glyceryl caprate coated with Curdlan encapsulating doxorubicin have also been developed with encapsulation yields of 2.8%, particle size less than 200 nm, and stability after one year of frozen storage[130].

Amphiphilic copolymers self assemble to form micellar structures applicable to drug delivery due to their drug loading capability and small size, taking advantage of the enhanced permeability and retention effect[2, 3]. Carboxymethylated Curdlan (CM-Curdlan) has been conjugated to sulfonylurea to create a grafted polymer with a hydrophillic backbone and hydrophobic sulfonylurea branches. All-*trans* Retinoic Acid (ATRA) was delivered from hydrogel nanoparticles to a hepatoma cell line by modification with lactobionic acid on the backbone of CM-Curdlan. Sonication was used to induce nanoparticle formation from water with drug loaded particle sizes of 181 nm. High encapsulation efficiencies and up to 50% drug release as studied by dialysis in saline was possible with first order release kinetics[33]. Curdlan copolymers have been developed with the conjugation of CM-Curdlan to cholesterol in order to encapsulate epirubicin via amphiphilic copolymer self-assembly initiated by probe sonication. A broader distribution in cells over the bare epirubicin was observed with no cytotoxicity[131].

2.5.3 Polynucleotide Complexes

In the last ten years, the development of polysaccharide-polynucleotide complexes has been of growing interest and especially so with 1,3-β-glucans that form hydrogen-bonded helical structures similar to the hydrogen bonds formed by polynucleotide chains in DNA. Nanoscale complexes formed between soluble 1,3-β-glucans and polynucleotides could be used therapeutically to provide a potent polynucleotide delivery system that also bears the pharmacological properties of 1,3-β-glucans. In 2000, using dextran, pullulan, and amylose with poly(C) caused no association as measured by circular dichroism spectra but lentinan and schizophyllan, water soluble 1,3-β-glucans showed a drastic change indicative of the formation of a complex. Insoluble 1,3-β-glucans such as Curdlan could not be used as they precipitated before any nanoscale complex could form[132]. Shortly after this finding with Curdlan, the polynucleotide complex was successfully formed by first carrying out a hydrolytic cleavage of the backbone to reduce the molecular weight[133]. More recently, the addition of solubilizing carbohydrate appendages through click chemistry to Curdlan has been an alternative route in utilizing Curdlan to bind poly(C)[134]. Using a similar chemical scheme, a positive ammonium group was grafted onto Curdlan to render it water soluble and capable to include a polynucleotide. In this instance, electrostatic interactions with the guest macromolecule were thought to assist the complexation[135]. The formation of the Curdlan-poly(C) complex was studied through semi-empirical molecular orbital calculations, demonstrating the presence of new hydrogen bonds between the host and guest and a unique deformation of the ribose sugar in the polynucleotide[34]. In addition, it has also now been demonstrated that the parallel arrangement of the two macromolecule chains in the complex is favoured[136]. Most of the work in this area has utilized homogeneous polynucleotides, as this has been found to be the only type of

polynucleotide capable of forming helical complexes. Recent work has generated the first potential applications of these findings with the development of a homogenous polynucleotide-appended anti-sense oligonucleotide to which a poly(ethylene glycol) (PEG) grafted schizophyllan copolymer could bind in a helical complex. The PEG grafts improved cellular uptake and reduced lysosomal degradation, allowing for successful demonstration of inhibited cell-growth through polynucleotide delivery[137, 138].

2.6 Future Research

1,3-β-glucans have enormous potential in a wide variety of fields due to their unique helix and gel forming capacity and potent pharmacological properties. As the literature simultaneously characterized the pharmacological effects and discovered the helical arrangements formed by these polysaccharides, two streams of research could be clearly identified: the first being the discovery of potential use of these polysaccharides in direct immunotherapeutic intervention for the treatment of cancers, healing of wounds, and impartation of microbial, fungal, and viral resistance and the second being the use of the helical gel structure beginning with the creation of food gels and now growing deeper into the development of nanostructures and encapsulation and release of active therapeutics. These two clearly defined streams will coalesce with a greater volume of research dedicated to applications such as drug delivery that utilize both the pharmacological and structure forming capabilities of 1,3-β-glucans.

3.0 Research Objectives

This thesis focuses on the development of improved drug delivery systems utilizing Curdlan. These systems differ from other polymer drug delivery systems because they bear the innate immunotherapeutic potential of 1,3-beta-glucans, making them multi-functional. From the literature, key works stand out in the history of Curdlan research such as the development of nanoparticle drug delivery systems[33, 129, 131], research into polynucleotide inclusion complexes[135], and the thermal gelation of Curdlan to create gel suppositories[127]. This thesis discusses significant contributions to the research on Curdlan drug delivery in both a nanoparticle form and as a hydrogel.

3.1 Polymer Nanoparticle Drug Delivery Objectives

For the development of polymer nanoparticles, Curdlan has not yet been used to its fullest potential. All applications of Curdlan in nanoparticle drug delivery thus far have utilized Curdlan as a water-stabilizing component. For example, a cholesterol-curdlan copolymer was developed wherein the cholesterol is hydrophobic and the Curdlan is relatively hydrophilic, allowing for micellar self-assembly to nanoparticles[131]. Again, a sulfonyl urea and Curdlan conjugate was made wherein Curdlan is once again the hydrophilic component, allowing for self assembly[33]. The problem with such an approach is that it does not utilize the natural hydrophobicity of Curdlan, which can yield drug association, and it exposes Curdlan on the surface of the particles. Since Curdlan interfaces with immune cells to provide its immunotherapeutic action, this architecture renders particles unable to be targeted to a specific site of action. To address this, a new copolymer nanoparticle platform has been developed where Curdlan is used as the central, hydrophobic core of the nanoparticle. Poly(ethylene glycol) (PEG) is used as the water stabilizing component of the copolymer. Doxorubicin, a hydrophobic,

chemotherapeutic drug is used as the model drug for the platform. This work is highly significant as a demonstration of Curdlan as a new platform for polymer nanoparticles where both the internal core of the system is both an attractor for the drug payload and an immunotherapeutic adjuvant.

Specific objectives for this work have been:

1. Synthesis of Curdlan-*graft*-PEG.
2. Spectroscopic validation of the new copolymer compound.
3. Light scattering evaluation of nanoparticle forming capacity.
4. Screening of the drug encapsulation capability.
5. Demonstration of the release of doxorubicin.

3.2 Hydrogel Drug Delivery Objectives

Since Curdlan thermal gels have already been demonstrated as a valid means to obtain controlled release suppositories[127] a new direction with hydrogel drug delivery systems was investigated using Curdlan. Curdlan has been highly successful in forming polynucleotide inclusion complexes with only simple chemical modification necessary to induce the formation of helical micelles[134, 135]. However, an inherent problem with these inclusion complexes is the fact that Curdlan only forms complexes with homogeneous polynucleotides at the molecular level, i.e. only one type of base nucleotide. This makes the phenomena uninteresting for gene delivery applications that attempt to deliver specific polynucleotide sequences. This issue has been partially overcome in the literature by first appending the useful polynucleotide with a section of homogeneous nucleotides to allow complex formation. This thesis describes an entirely different approach to creating Curdlan and DNA complexes, focusing on co-gelation of hydrogels instead of the formation of molecular complexes. The phenomena is dependent on the more recent discovery of the ability of Curdlan and DNA to form liquid crystalline gels (LCG)[123, 124, 126, 139]. Co-gelation allows the formation of a multi-phase LCG where the component Curdlan and polynucleotide partition into amorphous and crystalline phases. The hydrogel system is extremely flexible, being formed into different architectures across multiple length-scales from nanoparticles to macroscopic moldable cylinders. This provides ultimate flexibility in application from biologically implantable scaffolds to particulate delivery systems that allow the controlled release of polynucleotides. Controlled release is afforded through the use of a chelating agent to degrade the hydrogel structure.

The specific objectives for this component of the work were:

1. Develop a multi-phase LCG system using Curdlan and DNA as a macroscopic gel.

2. Evaluate the crystallinity of the LCG system using polarized light and the distribution of polynucleotides in the system.

3. Demonstrate the scale-down of the system to form smaller particles.

4. Evaluate the crystallinity of the scaled down system to ensure LCG behavior.

5. Further scale down the system to the micro-/nano-scale.

6. Evaluate the effect of processing parameters on architecture.

7. Investigate the release of polynucleotides from the LCG.

4.0 Synthesis of Curdlan-*graft*-Poly(ethylene glycol) and Formulation of Doxorubicin Loaded Core-Shell Nanoparticles

4.1 Introduction

This section of the thesis describes the synthesis of a Curdlan and PEG graft copolymer that has allowed the formation of core shell nanoparticles encapsulating doxorubicin in high yield. PEG (Fig. 13) has been used previously in Curdlan copolymers for the purpose of increasing cellular uptake and reducing lysosomal degradation of Curdlan-polynucleotide complexes[137, 138]. Doxorubicin (Fig. 13) was chosen as the model drug for this drug delivery platform due to its high hydrophobicity and cardiotoxicity, making it a current target for nanoparticle drug delivery[140, 141]. PEG has been used extensively in nanoparticle drug delivery as it acts to improve nanoparticle efficacy and pharmacokinetics *in vivo* by modulating protein adsorption[142-144]. The grafting was carried out by a dimethylaminopyridine (DMAP) mediated dicyclohexylcarbodiimide (DCC) ester forming mechanism, reacting the functional hydroxyls on the Curdlan backbone with a terminal carboxylic acid group on PEG (Fig. 14). Nanoprecipitation was used to formulate nanoparticles and Nuclear Magnetic Resonance (NMR), Dynamic Light Scattering (DLS), Transmission Electron Microscopy (TEM), and UV-visible spectrophotometry were used to characterize the system. The synthesized system is significant in the development of Curdlan-based immunotherapeutic drug delivery systems because it is the first to utilize the hydrophobicity of Curdlan to yield drug encapsulation and the first to incorporate Curdlan at the center of a nanoparticle where its immunogenicity leading to its immunotherapeutic properties is not exposed on the surface of the particle.

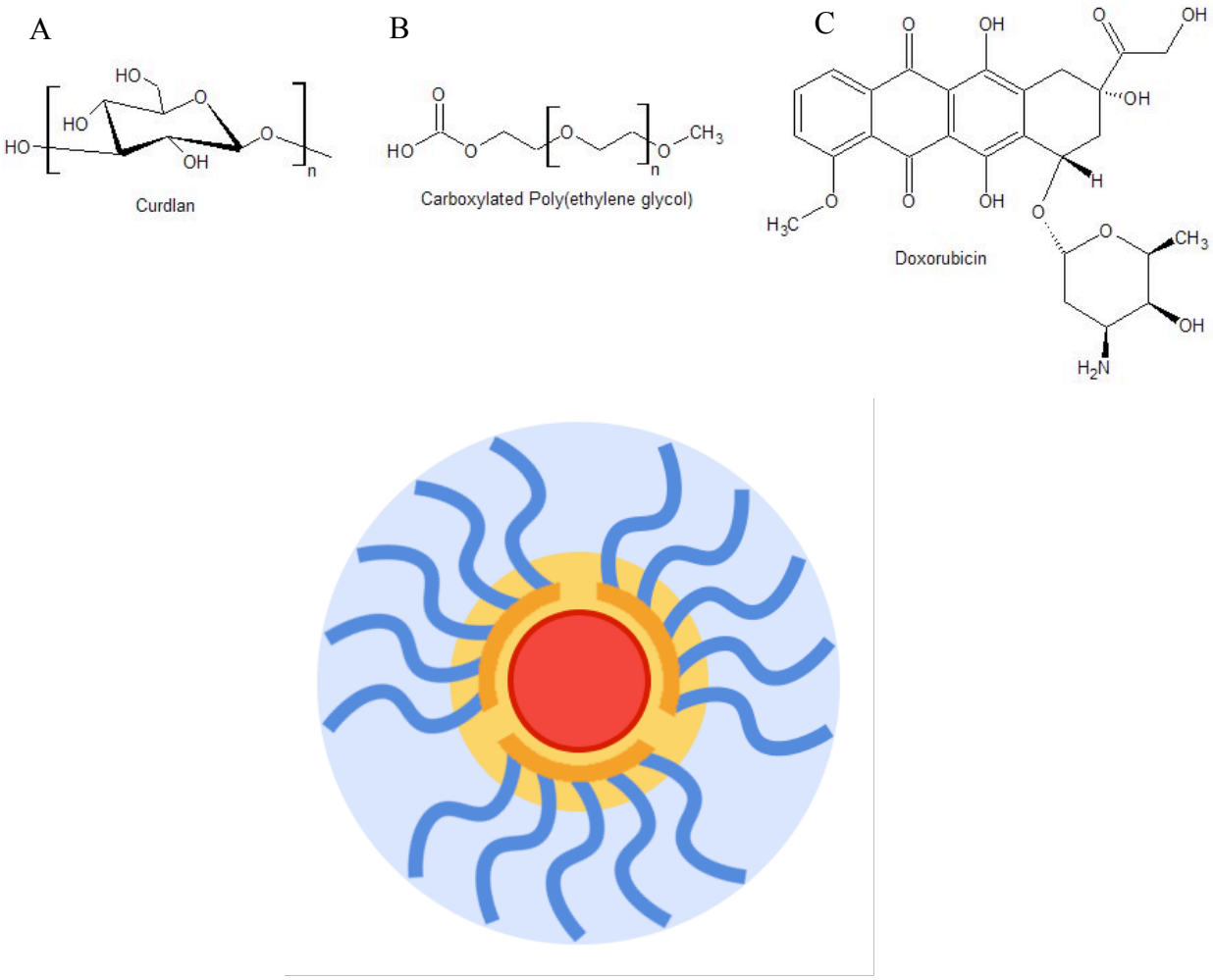

Figure 13. Components of the Nanoparticle and the Proposed Architecture. (Top) The developed system consists of PEG (**B**) grafted to Curdlan (**A**) encapsulating doxorubicin (**C**). **(Bottom)** A model of the nanoparticle architecture.

4.2 Experimental Methods

4.2.1 Materials

Raw Curdlan (~90 000 Da) was purchased from Wako Pure Chemical Industries and crushed with a mortar and pestle before use to aid dissolution. Monofunctional carboxylated PEG (~5000 Da) was purchased from NanoCS. Dicyclohexylcarbodiimide (DCC), dimethylaminopyridine (DMAP), and anhydrous dimethyl sulfoxide (DMSO) were purchased from Sigma Aldrich. All synthesis materials were used without further purification. Doxorubicin HCl was purchased from IntaTrade Chemicals GmbH and desalted according to the procedure described below. Amicon Filtration Units had a molecular weight cut-off (MWCO) of 10 000 Da and were purchased from Fisher Scientific.

4.2.2 Desalting of Doxorubicin Hydrochloride

Doxorubicin HCl was dissolved in distilled water at 4 mg/mL and 2 molar equivalents of triethylamine (TEA) were added and the solution vortex mixed until a color change to purple was observed. The solution was added to a separatory funnel and repeated portions of dichloromethane (DCM) were added. The bottom layer of DCM was removed and purged with compressed air at 50 °C. The obtained film was dissolved in DMSO at 6 mg/mL before use. The Doxorubicin-DMSO solution was serially diluted and tested in triplicate (300 μL each) in a 96 well microplate on a Biotek Epoch Microplate system at 480 nm to produce an absorbance-concentration calibration curve.

4.2.3 Synthesis of Curdlan-graft-Poly(ethylene glycol)

Curdlan (500 mg) was dissolved in 50 mL of stirring anhydrous DMSO under nitrogen bubbling for 1 hour. Simultaneously, carboxylated PEG (1 g) was dissolved in 30 mL of stirring

anhydrous DMSO at 60 °C under nitrogen bubbling for 20 minutes and DCC (600 mg) and DMAP (400 mg) were dissolved in 20 mL of stirring anhydrous DMSO under nitrogen bubbling for 20 minutes. DCC activated carboxylated PEG was formed by addition of the DCC/DMAP solution to the carboxylated PEG solution under stirring for 15 minutes. The activated carboxylated PEG solution was added to the Curdlan solution and stirred for 15 hours at room temperature. The final solution (100 mL) was added to 3.5 kDa MWCO dialysis tubing and dialyzed against 2 L of distilled water for 72 hours with water changed every 6-12 hours to remove unreacted PEG. The precipitated product was obtained by centrifugation with the water suspended over-grafted portion discarded. The product obtained from centrifugation was lyophilized overnight to remove water and washed 10 times with diethyl ether to remove DCC, DMAP, and dicyclohexyl urea. Residual ether was removed by desiccation to a dry powder consistency.

4.2.4 Determination of Nuclear Magnetic Resonance Spectra

All NMR Spectra were determined by dissolving 6.5 mg of polymer in 1 mL of DMSO-d6 under stirring for 30 minutes and scanning the sample on a 300 MHz Bruker NMR spectrometer. ^{1}H-NMR spectra were determined with 64 scans, ^{13}C-NMR spectra with 10 000 scans, and Heteronuclear Multiple Quantum Coherence (HMQC) spectra with 8 scans.

4.2.5 Preparation of Doxorubicin Loaded Curdlan-graft-PEG Nanoparticles

Curdlan-g-PEG was dissolved in DMSO at 7.5 mg/mL and varying volumes of polymer solution and 6 mg/mL Doxorubicin-DMSO solution were mixed at drug loading percentages (weight of doxorubicin/weight of polymer x 100) of 10, 20, and 40% each with a volume of 3.2 mL and a final polymer concentration of 3.5 mg/mL One milliliter of each solution was added in

a slow drop-wise manner to 10 mL of stirring distilled water with a mild vortex. The polymer droplet was allowed to disperse completely before addition of the next drop.

4.2.6 Dynamic Light Scattering

DLS results were obtained by removing 3 mL of the nanoparticle suspension to a 1 cm polystyrene cuvette and scanning in a Brookhaven 90 Plus Particle Size Analyzer with 2 scans of 20 minutes each. Number, volume, and intensity-weighted populations were used to quantify the particle size distribution.

4.2.7 Transmission Electron Microscopy

TEM samples were prepared by adding a single drop nanoparticle suspension onto a formvar coated copper grid and removing most of the drop using filter paper after 5 minutes. A single drop of 2% aqueous phosphotungstic acid was then added onto the grid for 50 seconds before being removed with filter paper to negatively stain the grid. TEM imaging was carried out on a Phillips CM10 Transmission Electron Microscope equipped with a lanthanum hexaboride filament saturated at an accelerating voltage of 60 kV.

4.2.8 Determination of Encapsulation Efficiency and Mass Yield of Doxorubicin

The suspension of doxorubicin loaded Curdan-g-PEG nanoparticles was concentrated in amicon filtration units at 4000 RPM for 20 minutes to remove water and free Doxorubicin and the retenate dissolved in 2 mL of DMSO by pipetting up and down vigorously. One milliliter of the resulting solution was diluted in 5 mL of DMSO and the sample was read in triplicate (100 μL) in a 96 well microplate at 480 nm. The absorbance was converted to concentration and the encapsulation efficiency determined by dividing the actual concentration by the ideal concentration. The mass yield was determined by normalizing the encapsulation efficiency by

the drug loading percentage. Displayed data is the average of three release runs with error bars displayed from the standard deviation.

4.2.9 In Vitro Release of Doxorubicin from Nanoparticles

Eleven milliliters of nanoparticle suspension in distilled water was added to a 3.5 kDa dialysis tube and dialyzed against 1.75L of distilled water for 3 hours to remove free drug. One mililiter of the washed nanoparticle suspension was added to 12.5 mL of distilled water and read in triplicate (100 μL) in a 96 well microplate at 480 nm to determine the 100% release condition. The remainder of the suspension in the dialysis tube (10 mL) was added into 125 mL of distilled water stirring at 37 °C. The release system was sealed with parafilm and covered in foil to avoid evaporation and doxorubicin degradation. Three 100 μL samples were taken at regular intervals and read in triplicate at 480 nm in a 96 well microplate. Constant volume was maintained in the release medium. Mean absorbance values were compared to the 100% release condition to determine the percent release. Displayed data is the average of three release runs with error bars displayed from the standard deviation.

4.3 Results and Discussion

The synthesis of Curdlan-g-PEG was carried out as shown in Figure 14 and verified by NMR spectroscopy. The Curdlan-g-PEG ^{1}H-NMR and ^{13}C-NMR spectra reveal new peaks at 3.47 ppm and 70.13 ppm respectively as well as some additional peaks in the 1.0-2.0 ppm range (Fig. 15) attributable to residual DCC difficult to remove by repeated ether washes. The two large signals present after dialysis and purification may be correlated to one another using HMQC analysis (Fig. 16) and correspond to the signals observed for NMR scans of the pure Carboxylated PEG and the literature for PEG derivatives[145]. Calculation of the degree of substitution is possible from comparison of the PEG and curdlan carbon peaks on the ^{13}C-NMR scan. Comparison of the intensities of the PEG and C(6) peaks yields a degree of substitution of 1.8 PEG chains per 100 glucopyranose units.

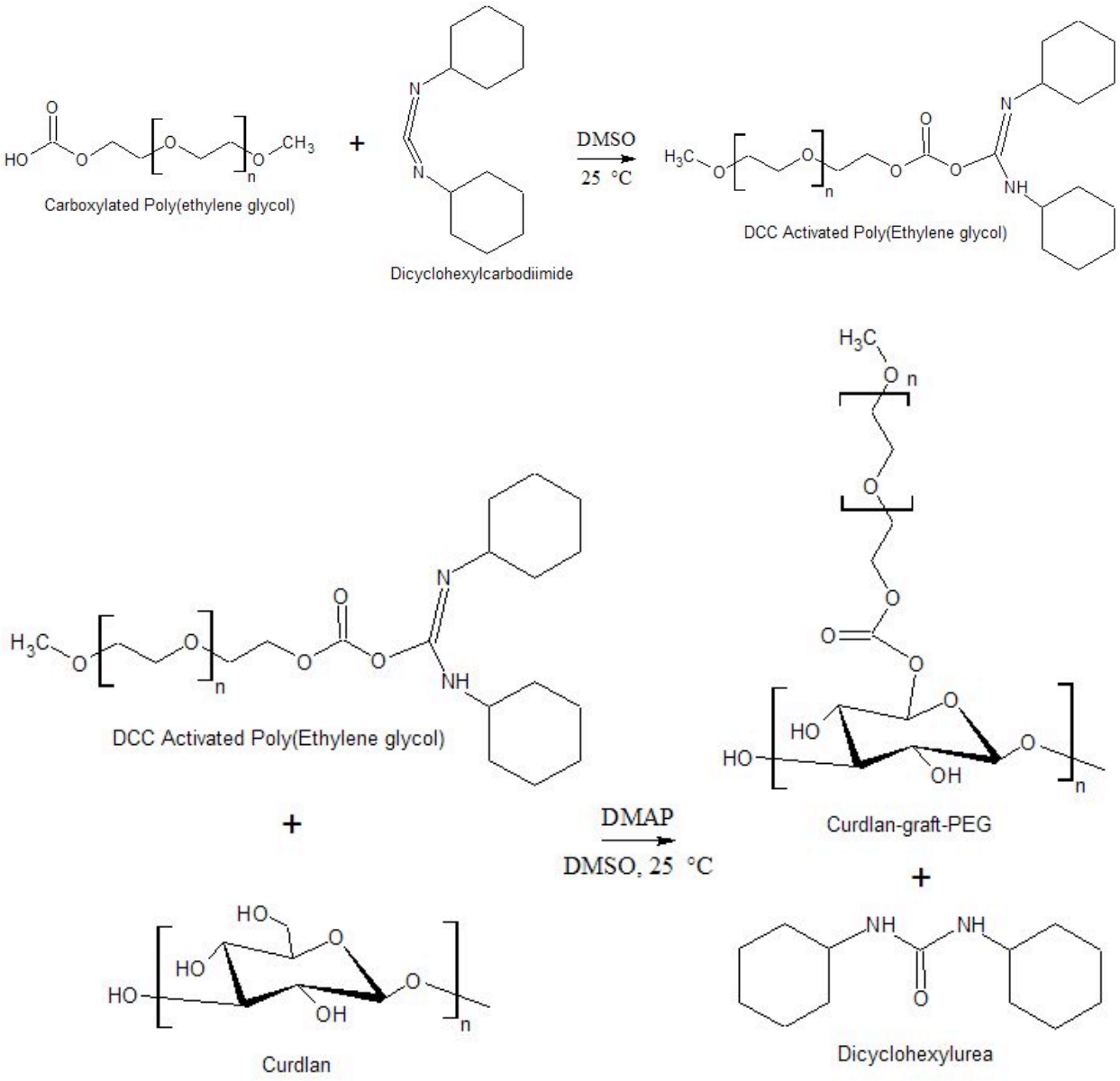

Figure 14. **Reaction Scheme for PEGylation of Curdlan. (Top)** Carboxylated PEG is reacted with DCC to produce the DCC-activated PEG derivative. **(Bottom)** Reaction of the activated PEG with Curdlan hydroxyls results in the stable ester graft and the formation of Dicyclohexylurea.

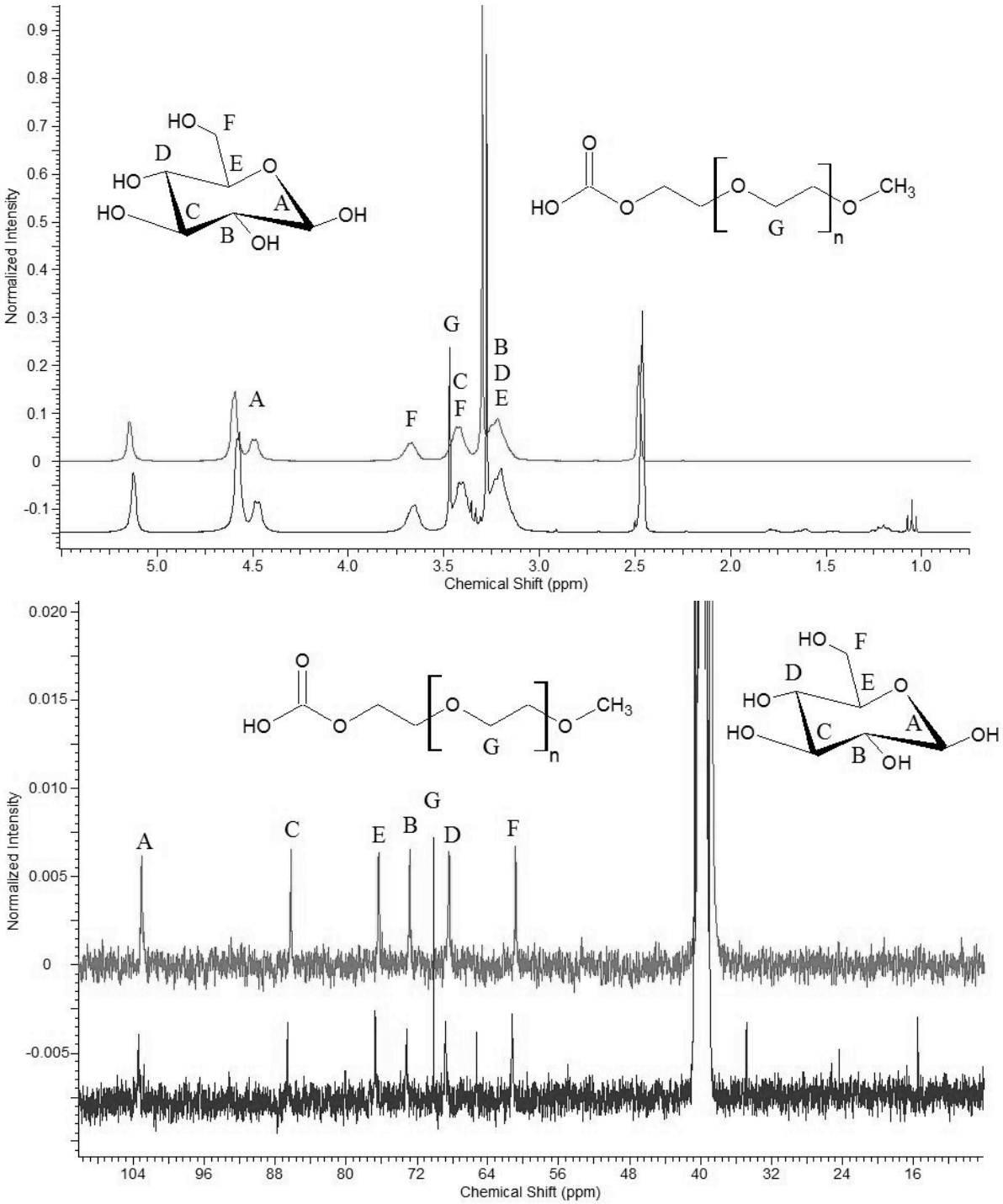

Figure 15. **Proton and Carbon NMR Spectra of Curdlan-g-PEG and Curdlan. (Top)** 1H-NMR scan of Curdlan **(Bottom)** and Curdlan-*graft*-PEG **(Top)** showing the presence of a significant PEG peak after grafting at 3.47 ppm. **(Bottom)** 13C-NMR scan of Curdlan **(Bottom)** and Curdlan-*graft*-PEG **(Top)** showing the PEG peak at 70.13 ppm.

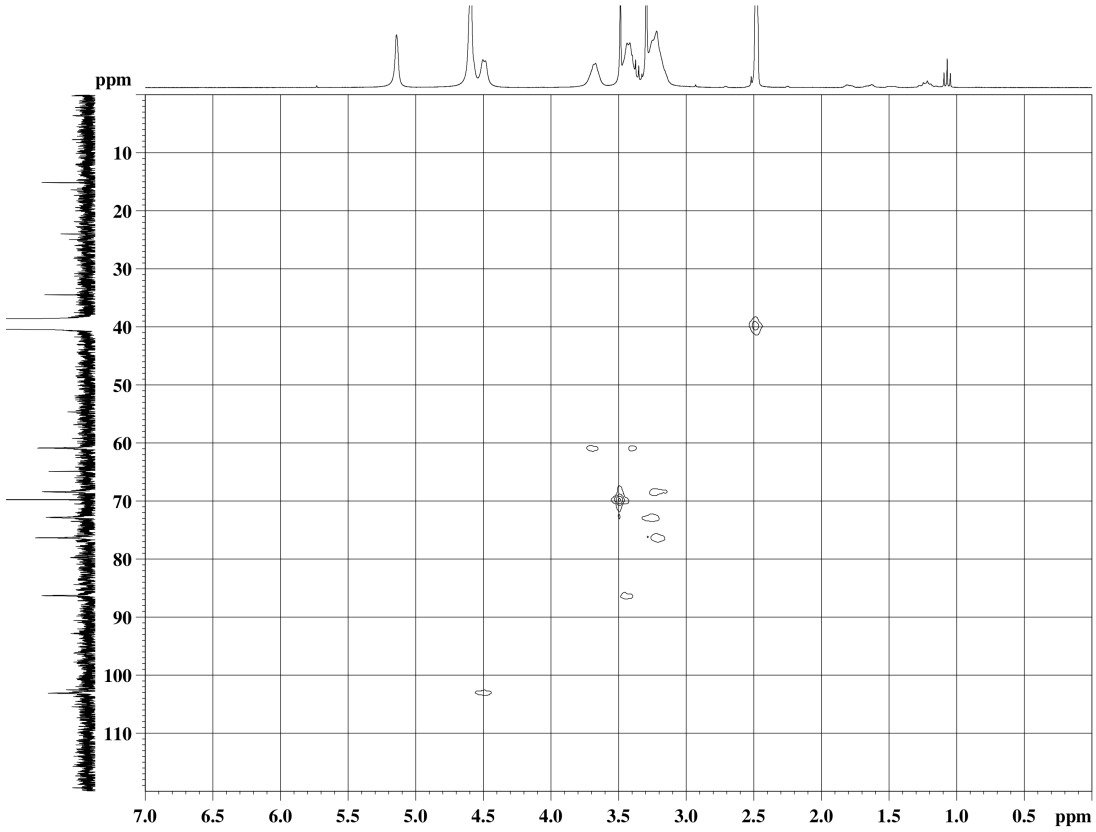

Figure 16. **HMQC scan of Curdlan-*graft*-PEG**. The correlation of six ^{13}C-NMR signals in the Curdlan ring to the ^{1}H-NMR signals and the correlation of the signals for PEG.

DLS analysis on empty and doxorubicin loaded Curdlan agglomerations and Curdlan-g-PEG nanoparticles formed by nanoprecipitation gave insight into the relative populations of particle sizes and the effect of PEGylation. With pure Curdlan and Doxorubicin agglomerations, DLS was inconclusive as the particle sizes were greater than the upper limit and the particles settled quickly in distilled water whereas number weighted DLS analysis of the Curdlan-g-PEG system revealed that PEGylation yielded stabled nanoparticles with a size of 93.1 nm (Fig. 17A) when Curdlan-g-PEG was loaded with 20% Doxorubicin compared to the empty particle size that averaged 53.3 nm. Nanoparticles were stable for greater than 7 days in distilled water. Intensity (Fig. 17B) and volume (Fig. 17D) weighted analysis revealed the presence of some

larger aggregations among the nanoparticles with particle sizes as high as 392.4 nm but these larger particles were not visible on TEM micrographs, suggesting they represent a minority in the population. The lognormal number population density (Fig. 17C) provides the nanoparticle size distribution with a mean particle size of 109.9 nm.

The initial drug loading percentage greatly affected the nanoparticle sizes determined by DLS. No difference was observed between 10% and 20% but 40% drug loading caused the particle size to increase to 400 nm and the particles to settle in distilled water. Since doxorubicin was capable of forming nanoparticles with particle sizes less than 75 nm at similar concentrations used in the polymer nanoparticles, the increased particle size over both free doxorubicin and free Curdlan-g-PEG suggested a coating of doxorubicin nanoparticles in the polymer as the main mechanism of interaction. It is postulated that the Curdlan-g-PEG aids aggregation of doxorubicin by providing a water stable coating but higher concentrations of doxorubicin yield particles that are too large to remain stable. The nanoparticle architecture is hypothesized to consist of a doxorubicin nanoparticle upon which the Curdlan backbone experiences hydrophobic interactions and PEG grafts align outwards to provide a water stable shell (Fig. 13).

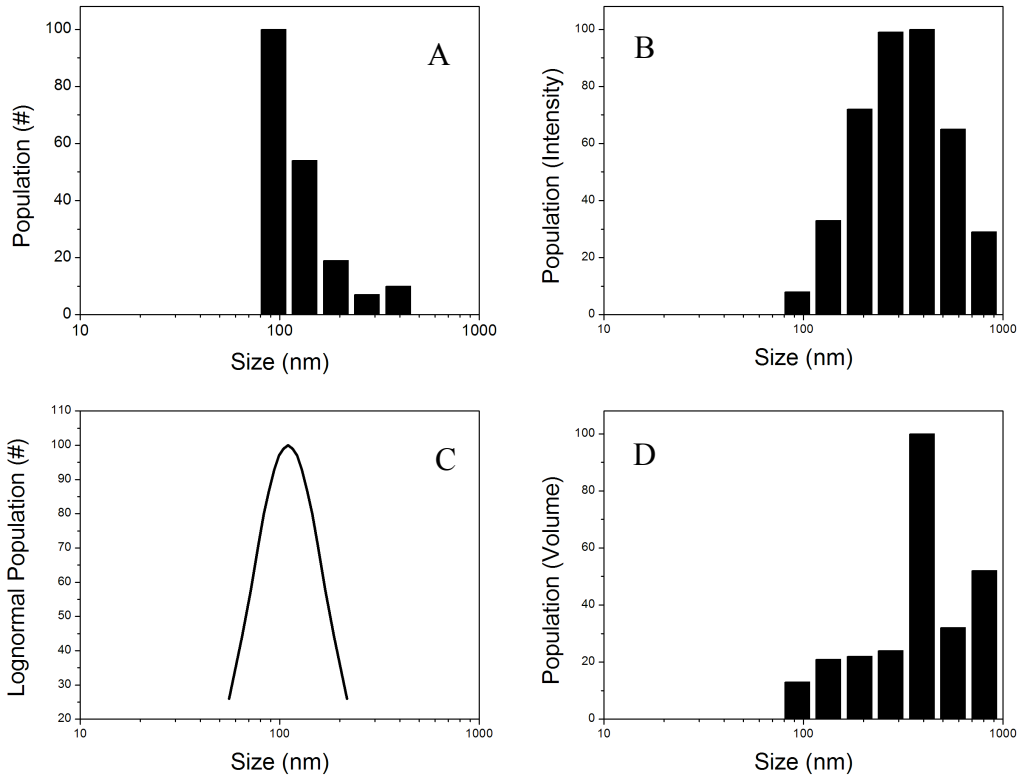

Figure 17. **DLS Study of Curdlan-g-PEG Nanoparticles. (A)** Number weighted population density for Curdlan-*graft*-PEG loaded with 20% Doxorubicin. **(B)** Intensity weighted population density. **(C)** Lognormal number population density. **(D)** Volume weighted population density.

TEM verified the particle sizes determined by DLS (Fig. 18) and the nanoparticle architecture proposed (Fig. 13B). Since the negative stain, phosphotungstic acid, used in the analysis is highly hydrophilic and electron dense, the hydrophilic PEG portion of the nanoparticles should appear darker due to increased electron density and doxorubicin and Curdlan portions of the nanoparticles should appear lighter. It was found that the presence of the doxorubicin center was clearly visible as bright white spots with a coating of a darker material (Fig 18A). No presence of bright white spots without such coating were visible on TEM samples, suggesting high encapsulation efficiency. Upon closer inspection of the nanoparticles the outer darker layer was found to consist of two layers itself (Fig 18B), with an inner lighter layer

postulated to be tightly packed curdlan backbone around the doxorubicin center and the outer darker layer fully extended PEG chains that provide water stability. Upon rudimentary calculation, the size of the dark PEG shell correlates well with the expected size of fully extended 5000 Da PEG chains. TEM thus correlates well with the nanoparticle architecture proposed (Fig. 13). In addition, TEM scans reveal the highest population of nanoparticles with a measurable size of 100 nm in close correlation with DLS results. Very few large aggregations, corresponding to larger scattering centers revealed by volume and intensity weighted DLS scans were observed.

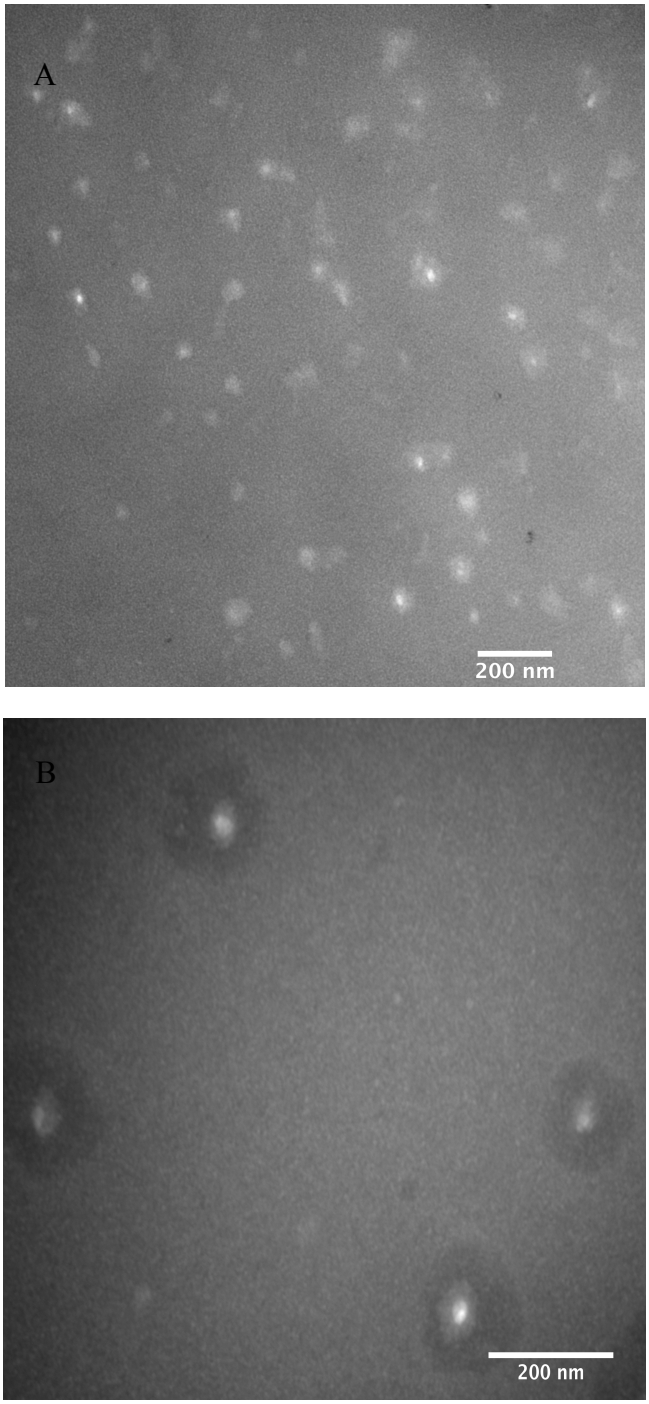

Figure 18. TEM Study of Curdlan-g-PEG Nanoparticles. (A) 20% Doxorubicin nanoparticles of Curdlan-*graft*-PEG appear as a bright Doxorubicin center with a coating of more electron dense material. **(B)** The coating is revealed to be multi layered with a compressed inner layer consisting mostly of Curdlan backbone and a looser outer layer consisting of extended PEG chains.

Doxorubicin loaded pure Curdlan and Curdlan-g-PEG nanoparticles were screened for encapsulation efficiency using UV-vis spectrophotometry. Prior to measurement, Doxorubicin not encapsulated was removed by Amicon centrifugation. The resulting retenate was dissolved in DMSO and diluted within an appropriate range for the calibration of the Doxorubicin. After determining the drug concentration and comparing to the ideal concentration, the encapsulation efficiencies for the varying drug loading percentages were determined for pure curdlan and Curdlan-g-PEG (Fig. 19). The Curdlan-g-PEG system attained similar encapsulation efficiencies as pure Curdlan. Therefore, PEGylation allowed for stable nanoparticle formation while maintaining the inherent drug encapsulating capability of pure Curdlan. Encapsulation efficiency is inherently dependent on the initial drug loading value and as such, this data was normalized by the drug loading percentages to determine the mass yield, a measure of the percentage of drug to polymer attained in the final suspension (Fig. 20). Since the nanoparticle system with 40% drug loading was unstable in water, the 20% loading condition is compared to other systems. The mass yield of 4-5% for the 20% loaded nanoparticle system is considerably high in comparison to other literature using Curdlan[130] and other encapsulation methods that typically produce mass yields around 2-3%[140] but the encapsulation efficiencies are significantly lower. Lower encapsulation efficiency can be explained by the need to use lower concentrations of Doxorubicin and polymer to enable nanoparticle formation by the nanoprecipitation method.

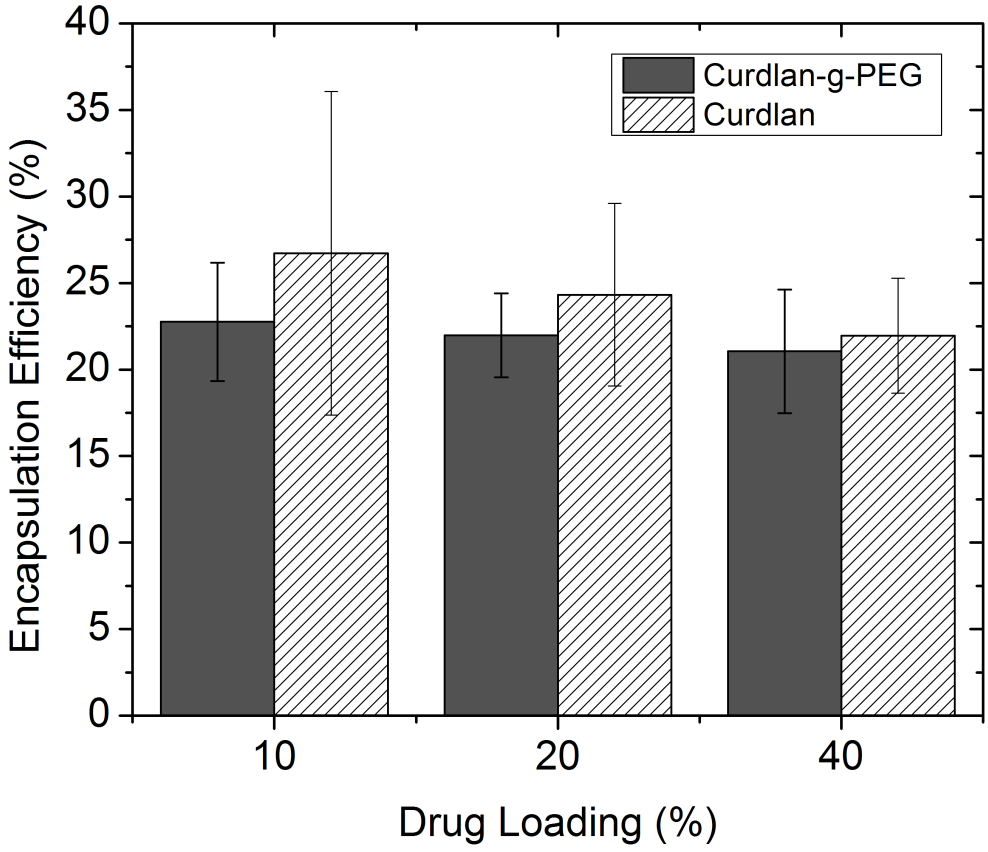

Figure 19. Encapsulation Efficiencies of Curdlan-*graft*-PEG and Pure Curdlan. The Curdlan system quickly aggregated and crashed upon precipitation and the Curdlan-*graft*-PEG system was stable indefinitely with similar encapsulation efficiency.

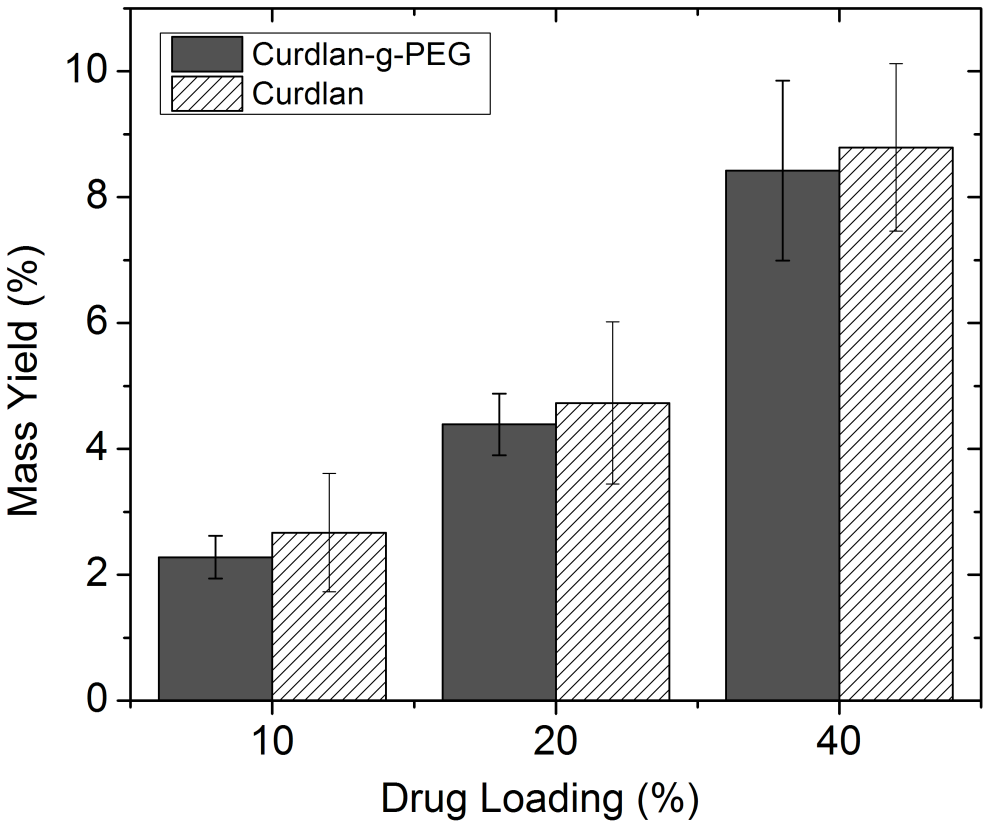

Figure 20. Mass yields of Curdlan-*graft*-PEG and Pure Curdlan. Encapsulation Efficiency normalized by the initial drug loading percentage.

In Vitro release was carried out in distilled water at 37 °C. The nanoparticles showed a release rate of nearly 100% of the releasable drug within 24 hours but during the initial wash to remove free drug, the nanoparticles became unstable. From this it can be concluded that the system was reliant on free Doxorubicin for stability although there were no visible coatings or networks of Doxorubicin on TEM micrographs to support this hypothesis. In addition to the reliance on Doxorubicin, the nature of the micelle constructed from graft copolymer means that the system is less amphiphilic than more commonly used block copolymer systems[140]. Consequently, it is postulated that, when exposed to the osmotic pressure of dialysis, the

nanoparticles have a tendency to break apart and aggregate into less ordered structures. Despite the issues with nanoparticle stability, it was possible to remove nearly 50% of the loaded doxorubicin as tested by UV-Vis spectrophotometry of periodically sampled distilled water from the release medium (Fig. 21). Experimentation with the degree of substitution to attain a better hydrophilic-lipophilic balance in the future could improve particle stability.

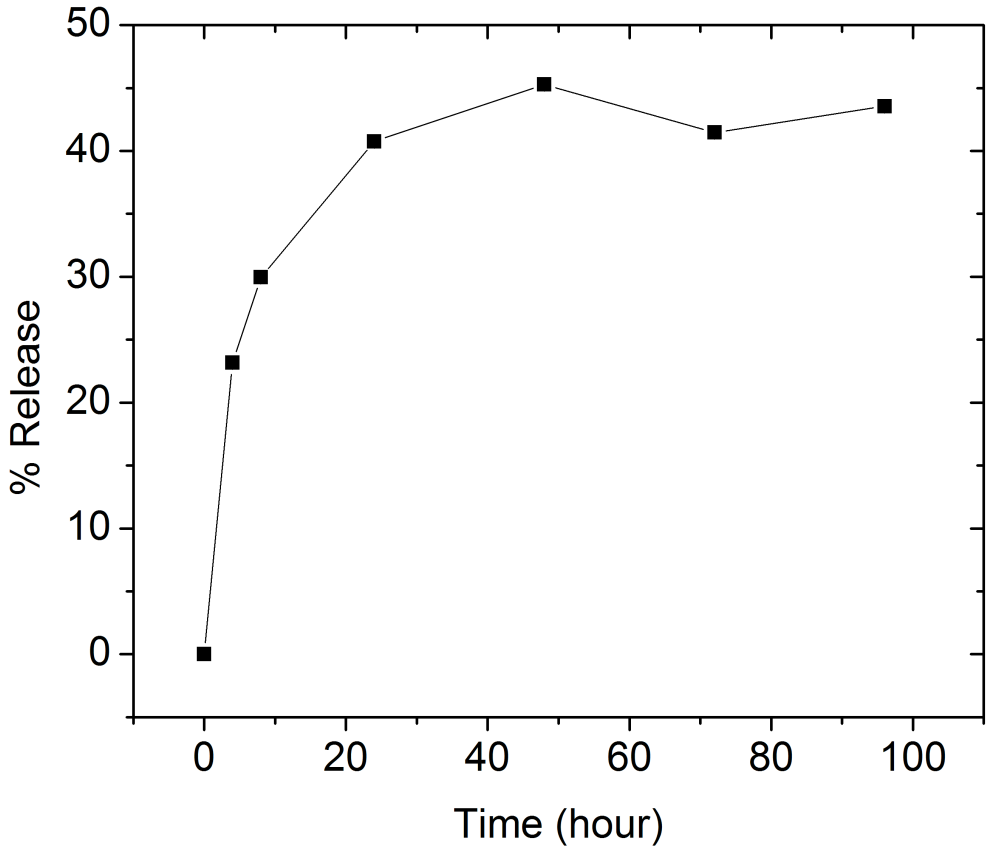

Figure 21. Release profile of Doxorubicin from Curdlan-*graft*-PEG nanoparticles.
Doxorubicin was released at a constant rate for 24 hours with a maximum release of 50%.

The developed nanoparticle system is a significant development in Curdlan nanoparticle systems as it is the first system to utilize a Curdlan copolymer wherein the hydrophobicity of Curdlan is used to create the drug association. Other systems have utilized sulfonylurea or cholesterol as the hydrophobic moiety and carboxymethylated curdlan as the water-stabilizing moiety[33, 131]. The Curdlan-g-PEG system developed herein may also be the first Curdlan nanoparticle system that could allow the transport of the immunomodulatory behavior of Curdlan to the site of a tumor as all other systems bear Curdlan on their surface, making them naturally immunogenic.

4.4 Conclusions

The present study demonstrated the feasibility of Curdlan-based nanoparticles for controlled drug release applications. A Curdlan-g-PEG copolymer was successfully synthesized by DMAP mediated DCC-ester formation using a monofunctional carboxylated PEG. A degree of substitution of 1.8 PEG chains per 100 glucopyranose units was obtained successfully. Nanoparticles with an average size of 109.9 nm were obtained with excellent stability in distilled water for greater than 7 days, demonstrating that PEGylation of curdlan can produce stable nanoparticles. The nanoparticle architecture appeared to be a central core of doxorubicin coated with a Curdlan backbone and fully extended PEG grafts in a triple layer structure. Encapsulation efficiencies comparable to pure Curdlan were obtained and high mass yields (4-5%) comparable to Curdlan solid lipid nanoparticles and well-recognized PLGA-PEG systems resulted. Doxorubicin released at a sustained rate for 24 hours. These results suggest that the PEGylated Curdlan is a viable approach to form nanoparticle delivery systems that may be useful in the

development of controlled release drug delivery applications that are also capable of providing immunotherapeutic action.

5.0 Formulation of Curdlan and DNA Multi-Phase Liquid Crystalline Gels

5.1 Introduction

This section of the thesis describes a new Curdlan hydrogel gene delivery platform that has allowed for triggered release of DNA from a hydrogel formed into a variety of shapes and sizes bearing the unique ability to partition crystalline and non-crystalline polymer and DNA. As described in section 3.0, this work is intended as a new approach that overcomes the need for homogenous polynucleotides in the formation of Curdlan gene delivery systems. Pure, unmodified Curdlan and double helical DNA isolated from salmon testes were chosen for this application. The use of unmodified Curdlan is an improvement over previous systems where the inherent water insolubility of Curdlan had to be overcome through functional grafts. Double helical salmon DNA was chosen as the model polynucleotide because it has very high molecular weight and would thus be most susceptible to crystallization. The LCG was formed by exposure of a mixture of Curdlan sodium hydroxide solution and aqueous DNA to aqueous calcium chloride. Macroscopic gels were formed using dialysis tubing and smaller structures were formed by drop-wise addition to stirring aqueous calcium chloride. The structures were characterized using polarized light to identify crystallinity, TEM to investigate smaller structures, and UV-visible spectrophometry to identify DNA concentrations via absorbance.

The present system is highly significant to Curdlan and gene delivery research as it allows the simultaneous co-gelation of DNA and Curdlan to form a gel shaped into a number of forms and sizes, capable of triggered release, and where the crystalline and non-crystalline phases of each material partition in the overall architecture. Partitioning amorphous material in the gel ensures that at least a portion of the payload DNA to remain in its amorphous state and avoid denaturation.

5.2 Experimental Methods

5.2.1 Materials

Curdlan (~90 kDa) was obtained from Wako Pure Chemical Industries. Sodium hydroxide was purchased from Caledon Laboratory chemicals, calcium chloride anhydrous salt, phosphotungstic acid (PTA), trisodium citrate salt and dialysis membrane were purchased from Fisher Scientific (Flat Width 45mm and 12,000 to 14,000 Da MWCO). DNA sodium salt (1300 kDa) from salmon testes was purchased from Sigma-Aldrich. Materials were used without further purification. Formvar coated transmission electron microscopy (TEM) grids were purchased from Canemco & Merivac (100 mesh copper grids). Linear polarizer sheets (2" x 2") were purchased from ThorLabs, Inc. and used to create the crossed nicols effect.

5.2.2 Macroscopic Cylindrical Gel Formation

Curdlan was dissolved in 0.4M sodium hydroxide solution at a concentration of 70 mg/mL (7% w/v). DNA was dissolved in deionized water at a concentration of 15 mg/mL (1.5% w/v). Aqueous DNA solution was mixed with Curdlan solution at different volume ratios to obtain 5%, 10% and 20% DNA/Curdlan samples. Thereafter, 12 mL of these solutions were added into a dialysis membrane, which was molded to form a cylindrical shape using two caps of diameter 29.6 mm. The dialysis tube was then immersed in 100 mL of 10% aqueous calcium chloride solution for 3 days. The gels were extracted by cutting out the dialysis membrane and cross-sectional slices of 5 mm were obtained for imaging. Imaging under visible light was carried out using a Sony Cyber-shot DSC-P150 digital camera. For polarized light analysis, two 2" x 2" linear polarizer sheets were placed orthogonal to each other on either side of the gel

cross-section to create crossed nicols. Images were taken using an Olympus PEN EPL-1 digital SLR camera.

5.2.3 DNA Concentration Profile

Cross-sectional gel slices used for imaging were further sliced longitudinally into 2 mm thin slices to determine the DNA distribution in the gel. The thin slices were dissolved in a 5% sodium citrate solution at a concentration of 10 mg/mL to chelate the calcium ions. The distribution of DNA in the gels was determined by adding 300 uL of the final solution in triplicate to a 96-well microplate and reading the absorbance at 260 nm on an Epoch UV-Vis spectrophometer.

5.2.4 Hydrogel Swelling

The swelling and drying capability of the gel was tested by leaving a piece of Curdlan gel in ambient air for 48 hours until the gel was completely dry and solid, losing 90% of its initial mass. The gel was then immersed in distilled water for 48 hours and subsequently re-dried to demonstrate another swelling cycle. To produce the swelling curve, the gel was measured every 24 hours using an analytical balance.

5.2.5 Spherical Gels

In order to formulate spherical gels of Curdlan and DNA, Curdlan was dissolved in 0.4M sodium hydroxide at a concentration of 15 mg/mL and DNA was dissolved in deionized water at a concentration of 15 mg/mL. These two solutions were mixed in various proportions to obtain samples of 0%, 25%, 50%, 75%, 100% DNA. This mixture was then slowly added drop-wise to magnetically stirring solution of 10 wt % aqueous calcium chloride. The solutions were allowed to stir for 1 hour. Gels were formed in the presence of DNA, with decreasing rigidity as DNA

concentration decreased. Pure Curdlan sample did not produce any visible structure. These samples were flattened between a microscope slide and a cover slip and imaged under 50x magnification on an Olympus BX-50 polarized light microscope.

5.2.6 Micro and Nano structures

Solutions of Curdlan and DNA were prepared at various concentrations, lower than previously used. These solutions were mixed in a 50/50 ratio and added to stirring 10% aqueous calcium chloride in a drop-wise manner. TEM samples were prepared by extracting a drop of sample onto the TEM grid and letting the polymer absorb for 3 minutes followed by filter paper blotting to remove excess solution. Staining was performed by exposing the samples to 2% PTA for 30 seconds. The samples were dried in ambient conditions overnight and imaged the following day. The most representative images were presented.

5.2.7 Triggered Release of DNA

The release characteristics of the DNA from the LCG were tested by exposing a slice of the 5% DNA macroscopic cylinder to either distilled water, 1% aqueous sodium citrate, or alternating between the two. Three hundred microliter samples were taken every 30 minutes and added in triplicate into a 96-well microplate and read at 260 nm on an Epoch UV-Vis spectrophotometer. The samples were replaced with fresh release medium. In the case of the alternating release medium, the medium was switched every 2 hours with a five-minute wash in distilled water upon each switch.

5.3 Results and Discussion

To begin investigation of co-gelation of Curdlan and DNA, macroscopic gel cylinders were formulated with DNA weight percentages of 0, 5, 10, and 20%. When the initial solution containing the appropriate mixture of Curdlan and DNA was exposed through dialysis to 10% aqueous calcium chloride for 3 days, calcium cations diffused into the polymer solution and cross-linked peripheral hydroxyls on the Curdlan monomers, leaving a concentration gradient of polymer from highest to lowest on the outside of the cylinder to the center[123]. Resilient LCG cylinders resulted with concentric turbid rings observable when the gel is sliced in cross-section. When the initial solution contained 1.5 wt % aqueous DNA, a similar gel was obtained with a different distribution of concentric rings. Figure 22 shows the different macroscopic cylindrical gels formed when cut into 5 mm cross-sections as well as the same gels viewed under double-polarized light (crossed nicols).

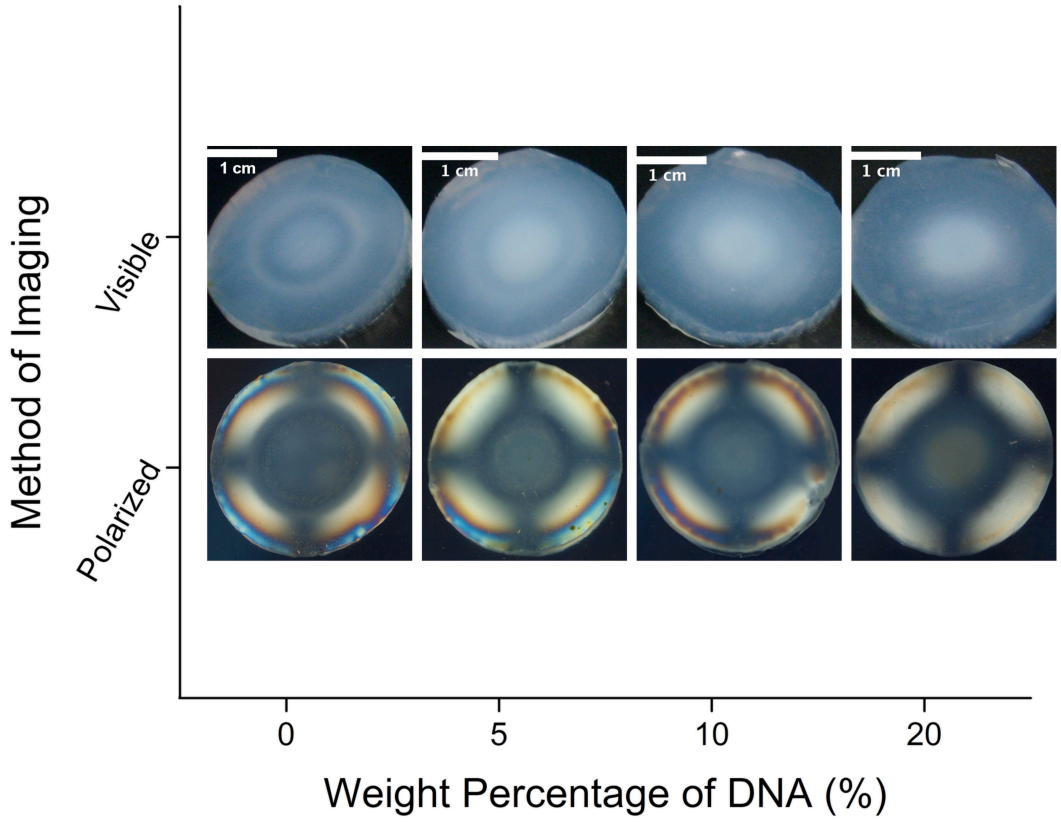

Figure 22. Curdlan and DNA Liquid Crystalline Gel Cylindrical Cross-sections. Concentrations are 100% Curdlan, 5% DNA, 10% DNA, and 20% DNA as seen through visible light **(Top)** and crossed nicols **(Bottom)**.

The pure Curdlan system showed characteristic concentric rings under visible light where the outer semi-transparent peripheral and inner semitransparent ring represented tightly packed LCG Curdlan and the white ring represented amorphous Curdlan[123]. When viewed under crossed nicols, the outer peripheral showed alternating colors characteristic of birefringence through an anisotropic crystal with the presence of orthogonal dark lines (isogyres) visible across the region. The presence of the dark isogyres and a lighter center of the gel demonstrated that, although similar in appearance to the amorphous ring under visible light, the region contained crystalline Curdlan. The gels formed by Dobashi[123] were thought to contain a lower density of Curdlan mesogens in the center due to the concentration gradient but these previously formed gels did not

have the white center observed. Since the molecular weight of the Curdlan in the present study was lower, compounded with the lower concentration in the center, less crystalline order may have resulted in the center of the present gel, causing visible light to be obscured and the white center to be present.

Introduction of DNA into the cylindrical gels caused a partitioning of the DNA into the amorphous and crystalline phases. Crystalline DNA formed a homogenous crystalline network with Curdlan along the periphery of the gels as seen by the darkening of the isogyre lines under crossed nicols, indicative of an anisotropic crystal. DNA was also present in an isotropic amorphous form as seen by darkening and expansion of the amorphous ring with increasing DNA concentration and loss of crystallinity previously indicated by the isogyres in the center of the gel. This behavior of DNA partitioning into anisotropic crystalline and isotropic amorphous has been observed in pure DNA LCG[139] and this remains in co-gelation with Curdlan.

To investigate the DNA profile in the gel to verify the conclusions from polarized light analysis, aqueous sodium citrate was used to dissolved longitudinal slices of the gel such that the DNA concentration could be tested by absorbance along multiple points of the gel radius. Using 2 mm slices and dissolving in sodium citrate at a constant concentration, absorbance at 260 nm reveals the profile for the different DNA weight percentages as shown in Figure 23.

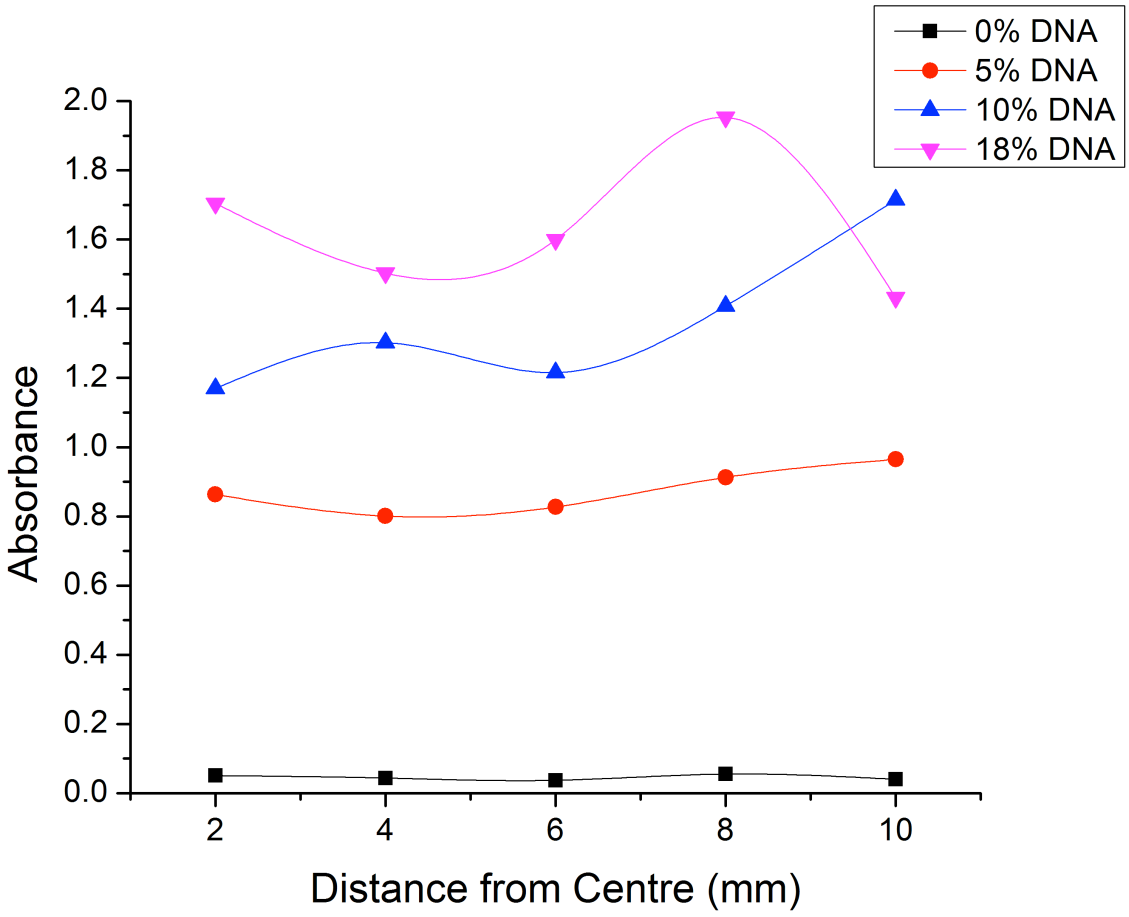

Figure 23. Concentration Profile of DNA in Cylindrical Gels. Absorbance at 260 nm of Longitudinal Gel Slices shown the presence of rings of DNA in the center and peripheral of the LCG.

The profile reveals that at DNA concentrations greater than 10% the presence of two concentrations of DNA is visible, representing the amorphous and crystalline phases observed under polarized light. The profile also confirms that the DNA and Curdlan form a homogeneous crystalline matrix as under both polarized light and visible light there is no visible partitioning in the peripheral of the gel but the DNA concentration is revealed to be high.

The swelling of the macroscopic gels was tested to verify the nature of the gel as a hydrogel, one that incorporates water into the matrix. After performing two drying and swelling cycles on the pure Curdlan sample, the result shown in Figure 24 below was obtained.

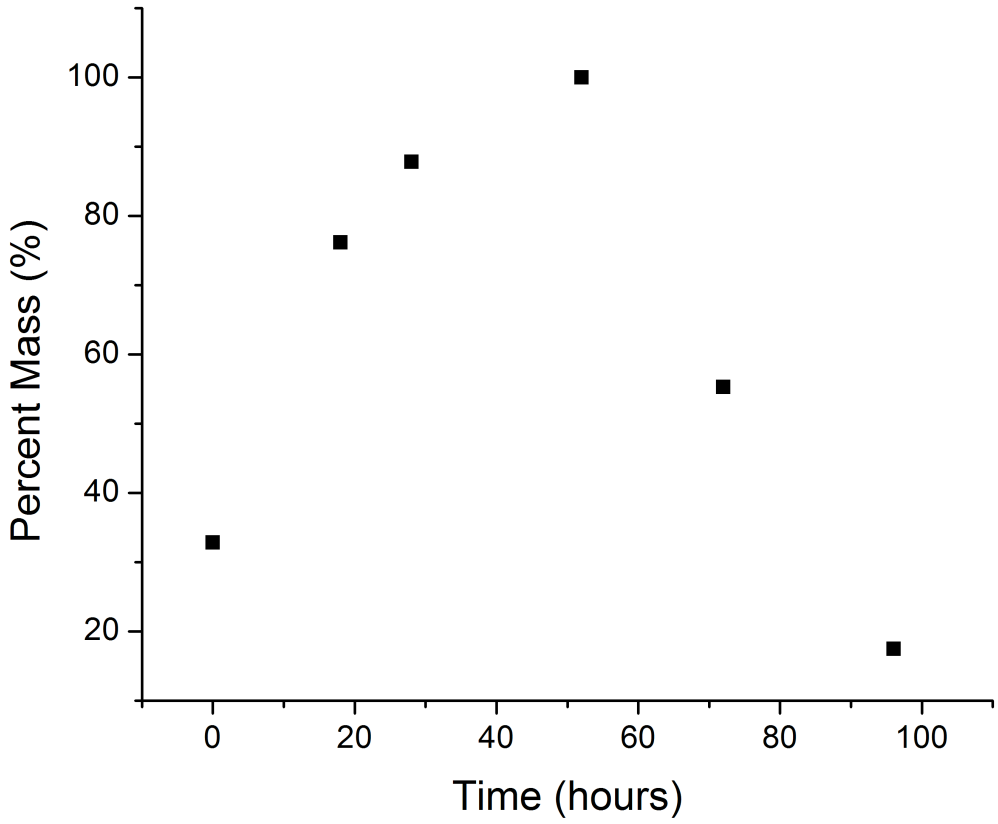

Figure 24. Swelling and Drying Characteristics of the Curdlan LCG.

The Curdlan LCG was capable of complete swelling after initial drying and was able to then return to a dried state of 10% of the initial weight, thereby demonstrating that the Curdlan LCG was indeed a hydrogel containing 90% water in its final structure.

Curdlan and DNA were also simultaneously gelled into elastic spherical gels on the millimeter length-scale when added drop-wise into stirring aqueous calcium chloride. Mixing

different ratios of Curdlan and DNA (100/0, 75/25, 50/50, 25/75, 0/100 DNA/Curdlan) caused the formation of markedly different structures. The 100/0 case caused the formation of tightly packed spherical precipitates whereas 75/25 and 50/50 cases yielded larger spherical gels that had a white center similar in appearance to the pure DNA and a semi-transparent outer coating of Curdlan. The 0/100 system was not capable of forming spherical gels. Figure 25 shows the spherical gels under visible and polarized light (crossed nicols).

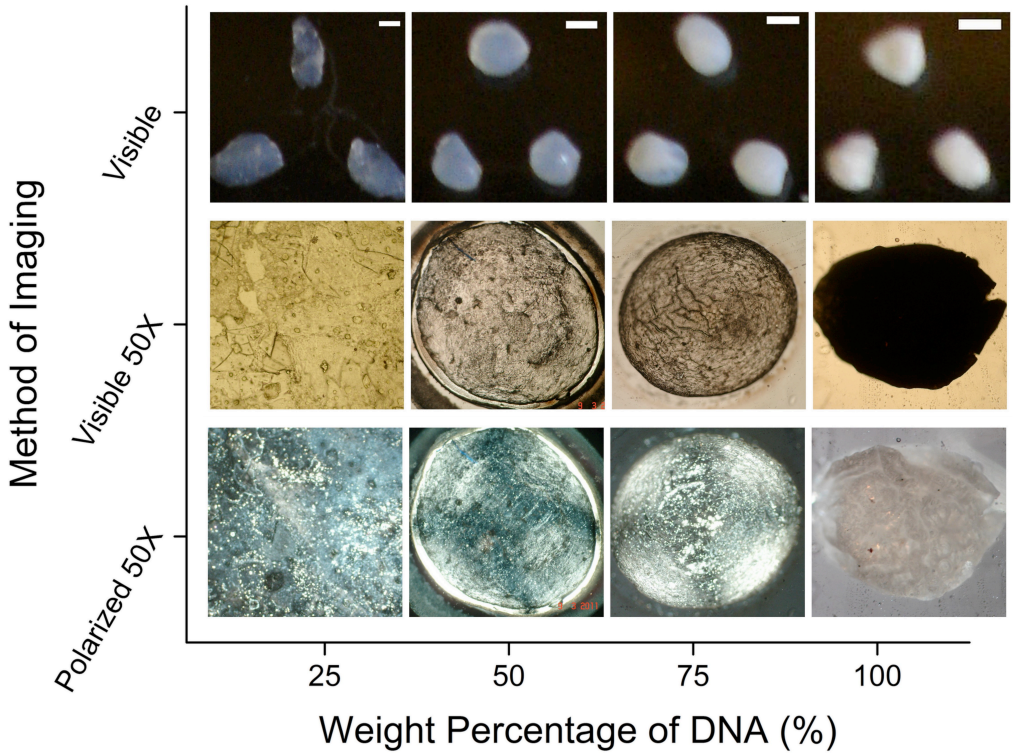

Figure 25. Curdlan and DNA Spherical Gels. Different concentrations of Curdlan and DNA as seen under visible light **(Top)** and polarized light **(Bottom)** Scale bars are 1mm.

The 100% DNA system formed a highly dense, optically opaque spherical gel. Under crossed nicols the system was revealed to be amorphous due to the lack of birefringence patterns. The structure was markedly different when 25% Curdlan was incorporated. No longer optically opaque, the gel showed the characteristic isogyre pattern representative of an anisotropic

crystalline structure. The center of the 75/25 gel under polarized light showed a blurring of the orthogonal isogyres, representative of a more isotropic, amorphous core. Further incorporation of Curdlan in the 50/50 sample caused a darkening of the isogyre pattern and more definition in the central region, characteristic of an overall increase in crystallinity. Therefore, the spherical gels are formed with 75/25 and 50/50 mixtures with a tendency for isotropic DNA to localize to the center and increasing levels of Curdlan to increase the overall crystallinity. In addition, the DNA acted as a nucleating center for the formation of the spherical gel as the pure Curdlan samples could not adequately hold their shape.

Lower concentrations of DNA allowed the formation of nano- and microstructures observable through TEM but not possible to screen for crystallinity using the concentional method. Using equal volumes of the Curdlan and DNA concentrations specified, the structures shown in Figure 26 were created.

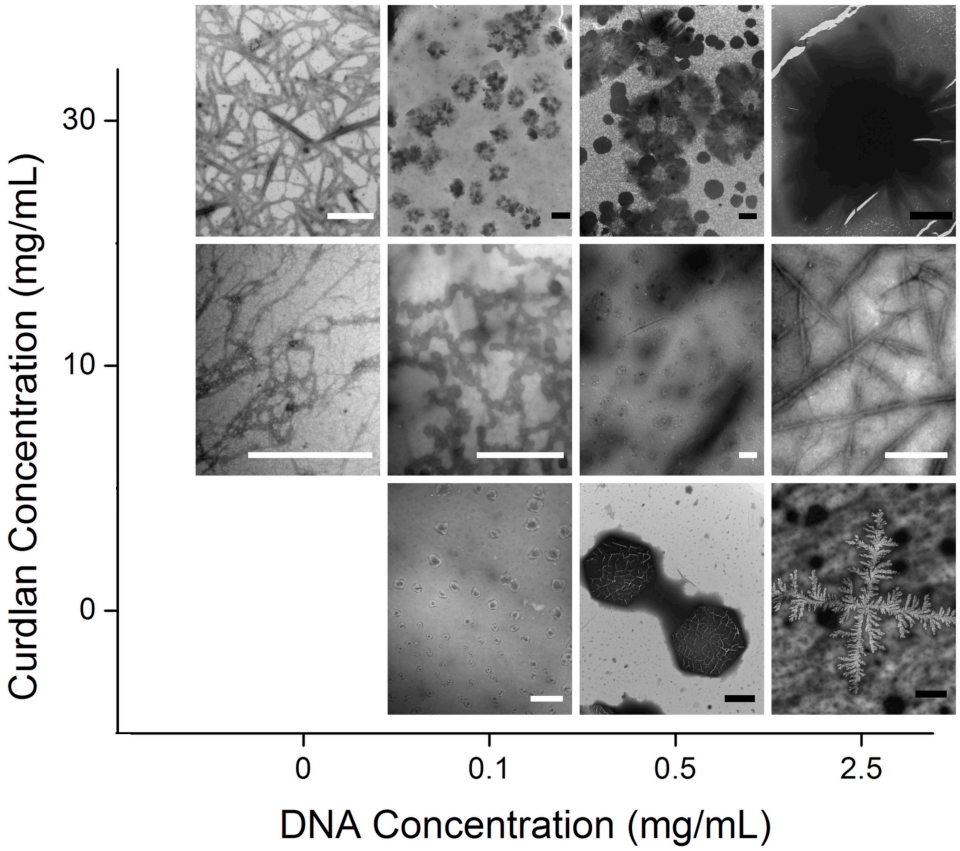

Figure 26. Curdlan and DNA nano- and micro-structures. Addition of equal volumes of Curdlan and DNA at different concentrations form a variety of structures. White scale bars are 500 nm and black scale bars are 2000 nm.

At the 30 mg/mL Curdlan level, TEM revealed the presence of a fibrous network of Curdlan with a fiber width of 20 nm. When repeated with 0.1 mg/mL DNA mixed in, 1.75 μm core-shell microparticles were observed with a white center and a dark outer ring. The white center was postulated to be a solid core of amorphous DNA and the outer ring more crystalline Curdlan due to the presence of fibrous striations on the periphery. This structure appeared to be the microscale analogue of the spherical gels. The ability to miniaturize the system was a remarkable phenomena. Introduction of higher concentrations of DNA caused a characteristic increase in the average microparticle size to 4 μm and upwards to 9-10 μm. At the 10 mg/mL Curdlan level, the pure Curdlan system showed a similar fibrous network with smaller features and a fiber diameter

of only 5-10 nm. Incorporation of DNA typically yielded the formation of particles and in the case of 0.1 mg/mL DNA, the presence of globular spheres within the fiber network was observed. Further increases in DNA concentration caused the formation of discrete nanoparticles with a fibrous nature and eventually the formation of a rigid rod-like structure wherein individual rods had a hydrophilic periphery and a hydrophobic core as observed by the contrast from PTA staining. Without Curdlan, DNA initially formed small particulates (200 nm). Higher concentrations of DNA caused the formation of highly crystalline structures beginning with hexagonal crystallites and evolving to DNA crystallites forming fractal patterns.

It was thus confirmed at the nanoscale that DNA acted as a nucleating center for the formation of particles. This was caused by its higher molecular weight leading to a higher rate of crystallization. After initial particle formation with DNA, the Curdlan could deposit on the surface as a stabilizing layer. In the case of lower concentrations of Curdlan where larger particles could not form, fibrous structures appeared to grow from the nucleating centers. With enough DNA, the nanoparticle-laden fibers evolved into rigid rods.

The ability to control the architecture of the LCG by simply changing concentration or altering the method of addition to aqueous calcium chloride allows the LCG system to be highly applicable to gene delivery. However, in order to be therapeutically relevant, the DNA had to be releasable in a bioactive state. As the absorbance of a DNA solution at 260 nm is representative of double helical DNA, the release of DNA was measured using spectrophotometry. Using the macroscopic gel cylinders as a convenient model for release, it was initially determined that no release of DNA occurred in distilled water as seen in Figure 27. This was a promising result as it allowed for investigation of controlled release phenomena.

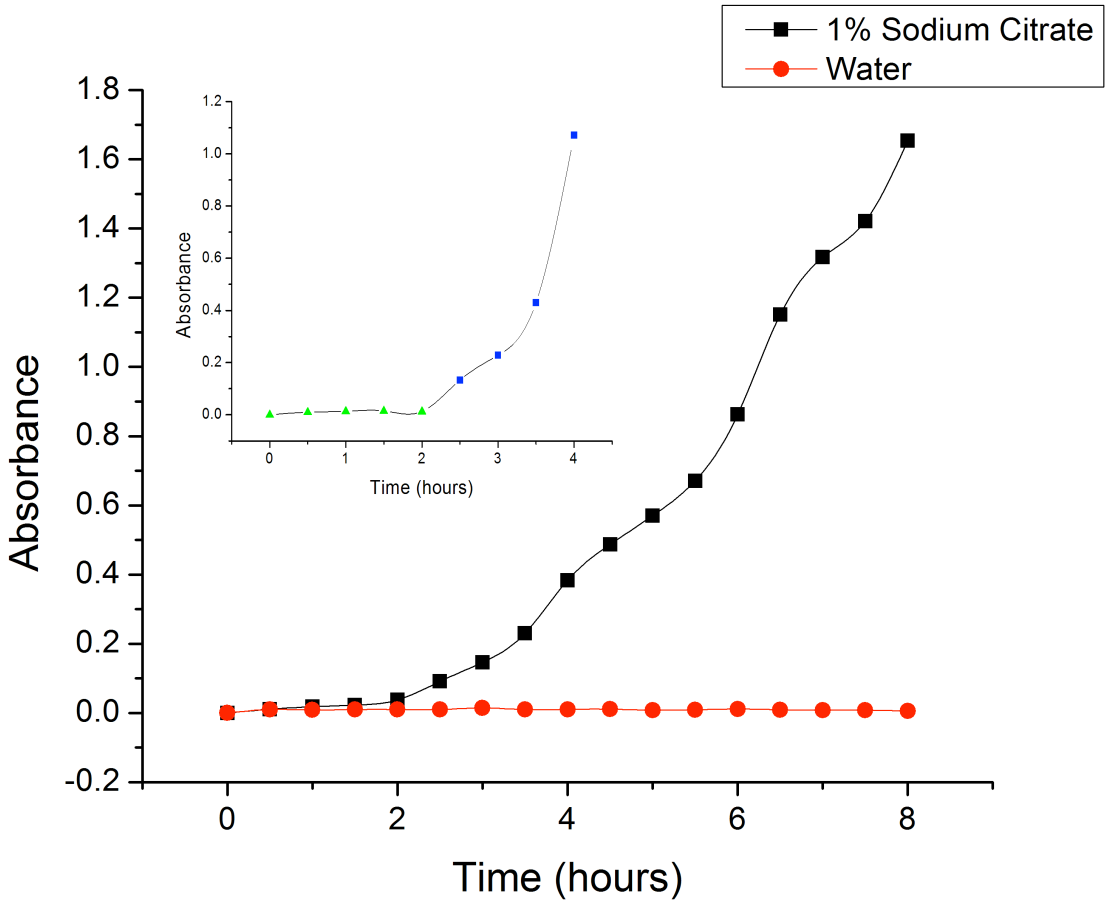

Figure 27. Triggered release of DNA from Curdlan/DNA Macroscopic Cylinders. Triggered release is possible in 1% sodium citrate and no release is observed in water. Inset plot shows the phenomena triggered on the same sample.

When another gel was exposed to 1% sodium citrate the release curve was drastically different. The sodium citrate caused chelation of the calcium cations, breaking the cross-links holding the hydrogel together. This phenomenon took two hours to begin allowing for both delayed and triggered release. It was possible to cause the triggered release effect from the same gel that had been hydrated in water as well, demonstrating that the gel must be hydrated for two hours before any release occurs, regardless of whether hydration occurs in water or the sodium citrate medium. As the gels dissolved completely after the release was completed, the release profile can be taken as percent release.

5.4 Conclusions

The demonstration of the co-gelation of Curdlan and DNA in the formation of unique structures ranging from nano- and microparticles to millimeter scale spherical gels and macroscopic cylinders controllable by concentration demonstrated the creation of a new multi-phase hydrogel system. Using the macroscopic cylinders, the nature of the system as a LCG was verified and the DNA profile showed the homogeneous crystallization of Curdlan and DNA. Since similar behavior was observed at the millimeter scale, it is believed that even the nano- and microscale systems are LCG's although this could not be proven using conventional means. The homogeneous crystallization of Curdlan and DNA down to the nanoscale demonstrated a new approach to forming polysaccharide-polynucleotide inclusion complexes.

6.0 Conclusions and Recommendations

6.1 Concluding Summary

This thesis began with an overview of the basics of drug delivery technologies and an introduction to polymer nanoparticles and hydrogels. A comprehensive literature review then introduced all the relevant work on Curdlan and 1,3-Beta-Glucans. Drawing from the research milestones applicable to drug delivery, research objectives were established to 1) Demonstrate the feasibility of Curdlan as the central core in a core-shell nanoparticle system through graft PEGylation and 2) Demonstrate the formation of a new type of hydrogel LCG that provided a new approach to Curdlan and polynucleotide inclusion complexes. Together, these objectives sought to establish Curdlan as a natural polysaccharide platform for drug delivery that could add a beneficial immunotherapeutic effect.

With the polymer nanoparticle system, PEG was successfully grafted onto Curdlan which allowed nanoparticle formation and the creation of a nanoparticle architecture with appropriate size to utilize the EPR effect for targeting and the ability to extract most of the encapsulated drug. Drawbacks of the system were instability during dialysis release. Despite this, Curdlan was successfully demonstrated as the core of a nanoparticle drug delivery system.

With the hydrogel LCG system, Curdlan and DNA were simultaneously gelled using calcium chloride to create macroscopic gel cylinders exhibiting LCG behavior and showing a unique partitioning of crystalline and amorphous material. The gel cylinders were evaluated to demonstrate that the structure contained 90% water and that the DNA formed a homogeneous crystalline network with Curdlan. The gels also both delayed and triggered release using sodium citrate as a chelating agent. The system was miniaturized to create spherical gels showing similar crystallinity phenomena to their macroscopic counterparts. Further miniaturization allowed the

demonstration of a suite of new architectures dependent on concentration ranging from nanofibers to microparticles. Overall, the research in this area was highly successful as it demonstrated a new type of multi-phase LCG and a new approach to forming Curdlan-polynucleotide drug delivery systems.

In terms of the overall trends in Curdlan research, two streams were observed in the literature review including 1) Research into the pharmacological applications of Curdlan using its potent immunotherapeutic effects and 2) Research into structural applications of Curdlan using the triple helical architecture to create structures ranging from resilient gels for food applications to nanoscale scaffolds for development various nanostructures. Drug delivery applications, especially those utilizing nanoscale phenomena were identified as an area where these two research streams coalesce.

With nanoparticle drug delivery systems now moving beyond clinical trials into wide spread use (ex. Doxil™ chemotherapeutic liposomes) it has been necessary to make use of the unique properties offered by natural polysaccharides in this field. Curdlan 1,3-Beta-Glucans, with their immense pharmacological potential, have been identified in the literature as a promising direction but until this present work Curdlan was not used to its fullest potential, being used only as a stabilizing agent. This work demonstrated that multi-functional Curdlan can exceed the capabilities of more common synthetic polymers such as Poly(lactic acid) for the purposes of nanoparticle drug delivery, thus contributing significantly to the advancement of the potential of Curdlan and the field of nanoparticle drug delivery.

The unique triple helical structures formed by Curdlan and other 1,3-Beta-Glucans have allowed for unique applications not attainable from synthetic polymers such as the formation of polynucleotide inclusion complexes. These unique helical structures have been shown to have

immense potential in gene delivery provided the limitation of requiring homogeneous polynucleotides is overcome. The presently discussed work has been highly significant in expanding the potential applications of Curdlan in gene delivery by expanding the array of methods to create inclusions complexes with polynucleotides using a crystallization approach as opposed to the commonly studied re-naturation approach.

6.2 Recommendations for Future Work

With the demonstration of Curdlan as a viable platform for polymer nanoparticle drug delivery, experimentation with the Curdlan-g-PEG system could be pursued further in order to obtain a better HLB that improves stability during drug release. As Curdlan has been demonstrated to be sufficiently hydrophobic for drug encapsulation the grafting of different hydrophilic moieties could produce more favorable results as well. The demonstration of polymer nanoparticle formation with a copolymer of Curdlan and water-soluble Dextran would be a milestone in the application of natural polysaccharides for polymer nanoparticle formation over synthetic polymers.

With the demonstration of the capability of Curdlan and DNA to form multi-phase hydrogel LCG it is possible to pursue a whole suite of new drug delivery systems using the co-gelation of Curdlan and DNA as opposed to the formation of molecular inclusion complexes. Investigation of the molecular weight effect would be the most important research direction, as the incorporation of smaller DNA strands would drastically change the nano- and microscale architectures observed. Additionally, new methods to expose the polymer solution to calcium chloride could allow for the formation of new structures. An example could be the use of a double emulsion scheme to allow for the formation of micro-droplets prior to exposure to calcium chloride. Such a system may not use DNA as a nucleating center and instead form a

homogeneous, solid microsphere. The successful research presented herein has been a demonstration of the potential of Curdlan as a new platform for a variety of drug delivery systems.

In summary, the significant works discussed herein could be built upon by:

1. Establishing an improved hydrophilic-lipophilic balance in the Curldan-g-PEG polymer by modulating the grafting frequency to improve nanoparticle stability.
2. Investigate the use of water-soluble natural polysaccharides to replace synthetic PEG to create a fully natural polymer system with improve stability.
3. Investigate the effect of molecular weight on the formation of nano- and microstructures in the formation of Curdlan and DNA LCG.
4. Discover new methods to expose Curdlan/DNA solution to calcium chloride (ex. Double emulsion) to create unique structures.

References

(1) Panyam, J.; Labhasetwar, V. Biodegradable nanoparticles for drug and gene delivery to cells and tissue. *Adv. Drug Deliv. Rev.* **2003***, 55*, 329-347.

(2) Maeda, H.; Wu, J.; Sawa, T.; Matsumura, Y.; Hori, K. Tumor vascular permeability and the EPR effect in macromolecular therapeutics: a review. *J. Controlled Release* **2000***, 65*, 271-284.

(3) Riess, G. Micellization of block copolymers. *Progress in Polymer Science* **2003***, 28*, 1107-1170.

(4) Rosler, A.; Vandermeulen, G. W. M.; Klok, H. A. Advanced drug delivery devices via self-assembly of amphiphilic block copolymers. *Adv. Drug Deliv. Rev.* **2001***, 53*, 95-108.

(5) Kataoka, K.; Harada, A.; Nagasaki, Y. Block copolymer micelles for drug delivery: design, characterization and biological significance. *Adv. Drug Deliv. Rev.* **2001***, 47*, 113-131.

(6) Kabanov, A. V.; Batrakova, E. V.; Alakhov, V. Y. Pluronic (R) block copolymers as novel polymer therapeutics for drug and gene delivery. *J. Controlled Release* **2002***, 82*, 189-212.

(7) Gregoriadis, G. Engineering liposomes for drug delivery: Progress and problems. *Trends Biotechnol.* **1995***, 13*, 527-537.

(8) Hamidi, M.; Azadi, A.; Rafiei, P. Hydrogel nanoparticles in drug delivery. *Adv. Drug Deliv. Rev.* **2008***, 60*, 1638-1649.

(9) Qiu, Y.; Park, K. Environment-sensitive hydrogels for drug delivery. *Adv. Drug Deliv. Rev.* **2001***, 53*, 321-339.

(10) Gombotz, W. R.; Wee, S. F. Protein release from alginate matrices. *Adv. Drug Deliv. Rev.* **1998***, 31*, 267-285.

(11) Czaja, W.; Krystynowicz, A.; Bielecki, S.; Brown, R. M. Microbial cellulose - the natural power to heal wounds. *Biomaterials* **2006***, 27*, 145-151.

(12) Lehr, C. M.; Bouwstra, J. A.; Schacht, E. H.; Junginger, H. E. Invitro Evaluation of Mucoadhesive Properties of Chitosan and some Other Natural Polymers. *Int. J. Pharm.* **1992***, 78*, 43-48.

(13) De Campos, A. M.; Sanchez, A.; Alonso, M. J. Chitosan nanoparticles: a new vehicle for the improvement of the delivery of drugs to the ocular surface. Application to cyclosporin A. *Int. J. Pharm.* **2001***, 224*, 159-168.

(14) Rowley, J. A.; Madlambayan, G.; Mooney, D. J. Alginate hydrogels as synthetic extracellular matrix materials. *Biomaterials* **1999***, 20*, 45-53.

(15) Wasser, S. P. Medicinal mushrooms as a source of antitumor and immunomodulating polysaccharides. *Appl. Microbiol. Biotechnol.* **2002***, 60*, 258-274.

(16) Sutherland, I. W. Microbial polysaccharides from Gram-negative bacteria. *Int. Dairy J.* **2001***, 11*, 663-674.

(17) Ruiz-Herrera, J.; Elorza, M. V.; Valentin, E.; Sentandreu, R. Molecular organization of the cell wall of Candida albicans and its relation to pathogenicity. *FEMS Yeast Res.* **2006***, 6*, 14-29.

(18) Chihara, G.; Hamuro, J.; Maeda, Y.; Arai, Y.; Fukuoka, F. Antitumour Polysaccharide Derived Chemically from Natural Glucan (Pachyman). *Nature* **1970***, 225*, 943-&.

(19) Sasaki, T.; Abiko, N.; Sugino, Y.; Nitta, K. Dependence on Chain-Length of Anti-Tumor Activity of (1-]3)-Beta-D-Glucan from Alcaligenes-Faecalis Var Myxogenes, Ifo 13140, and its Acid-Degraded Products. *Cancer Res.* **1978***, 38*, 379-383.

(20) Ohno, N.; Furukawa, M.; Miura, N. N.; Adachi, Y.; Motoi, M.; Yadomae, T. Antitumor beta-glucan from the cultured fruit body of Agaricus blazei. *Biol. Pharm. Bull.* **2001***, 24*, 820-828.

(21) Yano, T.; Matsuyama, H.; Mangindaan, R. E. P. Polysaccharide-Induced Protection of Carp, Cyprinus-Carpio L, Against Bacterial-Infection. *J. Fish Dis.* **1991***, 14*, 577-582.

(22) Rice, P. J.; Adams, E. L.; Ozment-Skelton, T.; Gonzalez, A. J.; Goldman, M. P.; Lockhart, B. E.; Barker, L. A.; Breuel, K. F.; DePonti, W. K.; Kalbfleisch, J. H.; Ensley, H. E.; Brown, G. D.; Gordon, S.; Williams, D. L. Oral delivery and gastrointestinal absorption of soluble glucans stimulate increased resistance to infectious challenge. *J. Pharmacol. Exp. Ther.* **2005***, 314*, 1079-1086.

(23) Ohno, N.; Suzuki, T.; Saito, K.; Yadomae, T. Enhancement of Clot Formation of Human Plasma by Beta-Glucans. *J. Pharmacobio-dyn.* **1990***, 13*, 525-532.

(24) Portera, C. A.; Love, E. J.; Memore, L.; Zhang, L. Y.; Muller, A.; Browder, W.; Williams, D. L. Effect of macrophage stimulation on collagen biosynthesis in the healing wound. *Am. Surg.* **1997***, 63*, 125-130.

(25) Wei, D.; Zhang, L. Y.; Williams, D. L.; Browder, W. Glucan stimulates human dermal fibroblast collagen biosynthesis through a nuclear factor-1 dependent mechanism. *Wound Repair Regen.* **2002***, 10*, 161-168.

(26) Bluhm, T. L.; Deslandes, Y.; Marchessault, R. H.; Perez, S.; Rinaudo, M. Solid-State and Solution Conformation of Scleroglucan. *Carbohydr. Res.* **1982***, 100*, 117-130.

(27) Deslandes, Y.; Marchessault, R. H.; Sarko, A. Packing Analysis of Carbohydrates and Polysaccharides .13. Triple-Helical Structure of (1-]3)-Beta-D-Glucan. *Macromolecules* **1980***, 13*, 1466-1471.

(28) Chuah, C. T.; Sarko, A.; Deslandes, Y.; Marchessault, R. H. Packing Analysis of Carbohydrates and Polysaccharides .14. Triple-Helical Crystalline-Structure of Curdlan and Paramylon Hydrates. *Macromolecules* **1983***, 16*, 1375-1382.

(29) Nakao, Y.; Konno, A.; Taguchi, T.; Tawada, T.; Kasai, H.; Toda, J.; Terasaki, M. Curdlan - Properties and Application to Foods. *J. Food Sci.* **1991***, 56*, 769-&.

(30) Funami, T.; Funami, M.; Tawada, T.; Nakao, Y. Decreasing oil uptake of doughnuts during deep-fat frying using curdlan. *J. Food Sci.* **1999**, *64*, 883-888.

(31) Bohn, J. A.; BeMiller, J. N. (1->3)-beta-D-glucans as biological response modifiers: A review of structure-functional activity relationships. *Carbohydr. Polym.* **1995**, *28*, 3-14.

(32) Liu, J.; Gunn, L.; Hansen, R.; Yan, J. Combined yeast-derived beta-glucan with anti-tumor monoclonal antibody for cancer immunotherapy. *Exp. Mol. Pathol.* **2009**, *86*, 208-214.

(33) Na, K.; Park, K. H.; Kim, S. W.; Bae, Y. H. Self-assembled hydrogel nanoparticles from curdlan derivatives: characterization, anti-cancer drug release and interaction with a hepatoma cell line (HepG2). *J. Controlled Release* **2000**, *69*, 225-236.

(34) Miyoshi, K.; Uezu, K.; Sakurai, K.; Shinkai, S. Polysaccharide-polynucleotide complexes. Part 32. Structural analysis of the Curdlan/poly(cytidylic acid) complex with semiempirical molecular orbital calculations. *Biomacromolecules* **2005**, *6*, 1540-1546.

(35) Hasegawa, T.; Fujisawa, T.; Numata, M.; Li, C.; Bae, A. H.; Haraguchi, S.; Sakurai, K.; Shinkai, S. Schizophyllan acts as a one-dimensional host to accommodate 5,10,15,20-tetrakis(4-carboxyphenyl)porphyrinatozinc acetate to produce its fibrous superstructure. *Chem. Lett.* **2005**, *34*, 1118-1119.

(36) Haraguchi, S.; Hasegawa, T.; Numata, M.; Fujiki, M.; Uezu, K.; Sakurai, K.; Shinkai, S. Oligosilane-nanofibers can be prepared through fabrication of permethyldecasilane within a helical superstructure of schizophyllan. *Org. Lett.* **2005**, *7*, 5605-5608.

(37) Harada, T.; Yoshimura, T. Production of New Acidic Polysaccharide Containing Succinic Acid by Soil Bacterium. *Biochim. Biophys. Acta* **1964**, *83*, 374-&.

(38) Harada, T.; Masada, M.; Fujimori, K.; Maeda, I. Production of a Firm Resilient Gel-Forming Polysaccharide by a Mutant of Alcaligenes Faecalis Var Myxogenes 10c3. *Agric. Biol. Chem.* **1966**, *30*, 196-&.

(39) Harada, T.; Misaki, A.; Saito, H. Curdlan - a Bacterial Gel-Forming Beta-1 3-Glucan. *Arch. Biochem. Biophys.* **1968**, *124*, 292-&.

(40) Maeda, I.; Saito, H.; Masada, M.; Misaki, A.; Harada, T. Properties of Gels Formed by Heat Treatment of Curdlan a Bacterial Beta-1,3 Glucan. *Agric. Biol. Chem.* **1967**, *31*, 1184-&.

(41) Zhang, H. B.; Nishinari, K.; Williams, M. A. K.; Foster, T. J.; Norton, I. T. A molecular description of the gelation mechanism of curdlan. *Int. J. Biol. Macromol.* **2002**, *30*, 7-16.

(42) Sundaral.M Some Aspects of Stereochemistry and Hydrogen Bonding of Carbohydrate Related to Polysaccharide Conformations. *Biopolymers* **1968**, *6*, 189-&.

(43) Saito, H.; Ohki, T.; Sasaki, T. C-13 Nuclear Magnetic-Resonance Study of Gel-Forming (1-]3)-Beta-D-Glucans - Evidence of Presence of Single-Helical Conformation in a Resilient Gel of a Curdlan-Type Polysaccharide-13140 from Alcaligenes-Faecalis-Var-Myxogenes-Ifo13140. *Biochemistry (N. Y.)* **1977**, *16*, 908-914.

(44) Miyoshi, K.; Uezu, K.; Sakurai, K.; Shinkai, S. Proposal of a new hydrogen-bonding form to maintain curdlan triple helix. *Chem. Biodivers.* **2004**, *1*, 916-924.

(45) Gagnon, M.; Lafleur, M. From curdlan powder to the triple helix gel structure: An attenuated total reflection-infrared study of the gelation process. *Appl. Spectrosc.* **2007**, *61*, 374-378.

(46) Harada, T.; Koreeda, A.; Sato, S.; Kasai, N. Electron-Microscopic Study on the Ultrastructure of Curdlan Gel - Assembly and Dissociation of Fibrils by Heating. *J. Electron Microsc.* **1979**, *28*, 147-153.

(47) Tada, T.; Tamai, N.; Matsumoto, T.; Masuda, T. Network structure of curdlan in DMSO and mixture of DMSO and water. *Biopolymers* **2001**, *58*, 129-137.

(48) Tada, T.; Matsumoto, T.; Masuda, T. Influence of alkaline concentration on molecular association structure and viscoelastic properties of curdlan aqueous systems. *Biopolymers* **1997**, *42*, 479-487.

(49) Konno, A.; Harada, T. Thermal-Properties of Curdlan in Aqueous Suspension and Curdlan Gel. *Food Hydrocoll.* **1991**, *5*, 427-434.

(50) Ikeda, S.; Shishido, Y. Atomic force microscopy studies on heat-induced gelation of Curdlan. *J. Agric. Food Chem.* **2005**, *53*, 786-791.

(51) Zhang, L.; Wang, C.; Cui, S. X.; Wang, Z. Q.; Zhang, X. Single-molecule force spectroscopy on curdlan: Unwinding helical structures and random coils. *Nano Lett.* **2003**, *3*, 1119-1124.

(52) McIntire, T. M.; Brant, D. A. Observations of the (1 -> 3)-beta-D-glucan linear triple helix to macrocycle interconversion using noncontact atomic force microscopy. *J. Am. Chem. Soc.* **1998**, *120*, 6909-6919.

(53) Pillemer, L.; Blum, L.; Lepow, I. H.; Ross, O. A.; Todd, E. W.; Wardlaw, A. C. The Properdin System and Immunity .1. Demonstration and Isolation of a New Serum Protein, Properdin, and its Role in Immune Phenomena. *Science* **1954**, *120*, 279-285.

(54) Brade, V.; Lee, G. D.; Nicholso.a; Shin, H. S.; Mayer, M. M. Reaction of Zymosan with Properdin System in Normal and C4-Deficient Guinea-Pig Serum - Demonstration of C3-Cleaving and C5-Cleaving Multi-Unit Enzymes, both Containing Factor-B, and Acceleration of their Formation by Classical Complement Pathway. *J. Immunol.* **1973**, *111*, 1389-1400.

(55) Hamuro, J.; Hadding, U.; Bittersuermann, D. Solid-Phase Activation of Alternative Pathway of Complement by Beta-1,3-Glucans and its Possible Role for Tumor Regressing Activity. *Immunology* **1978**, *34*, 695-705.

(56) Riggi, S. J.; Diluzio, N. R. Identification of a Reticuloendothelial Stimulating Agent in Zymosan. *Am. J. Physiol.* **1961**, *200*, 297-&.

(57) Czop, J. K. The Role of Beta-Glucan Receptors on Blood and Tissue Leukocytes in Phagocytosis and Metabolic-Activation. *Pathol. Immunopathol. Res.* **1986**, *5*, 286-296.

(58) Vetvicka, V.; Thornton, B. P.; Ross, G. D. Soluble beta-glucan polysaccharide binding to the lectin site of neutrophil or natural killer cell complement receptor type 3 (CD11b/CD18) generates a primed state of the receptor capable of mediating cytotoxicity of iC3b-opsonized target cells. *J. Clin. Invest.* **1996**, *98*, 50-61.

(59) Brown, G. D.; Taylor, P. R.; Reid, D. M.; Willment, J. A.; Williams, D. L.; Martinez-Pomares, L.; Wong, S. Y. C.; Gordon, S. Dectin-1 is a major beta-glucan receptor on macrophages. *J. Exp. Med.* **2002**, *196*, 407-412.

(60) Brown, G. D.; Herre, J.; Williams, D. L.; Willment, J. A.; Marshall, A. S. J.; Gordon, S. Dectin-1 mediates the biological effects of beta-glucans. *J. Exp. Med.* **2003**, *197*, 1119-1124.

(61) van Bruggen, R.; Drewniak, A.; Jansen, M.; van Houdt, M.; Roos, D.; Chapel, H.; Verhoeven, A. J.; Kuijpers, T. W. Complement receptor 3, not Dectin-1, is the major receptor on human neutrophils for beta-glucan-bearing particles. *Mol. Immunol.* **2009**, *47*, 575-581.

(62) Ross, G. D.; Vetvicka, V.; Yan, J.; Xia, Y.; Vetvickova, J. Therapeutic intervention with complement and beta-glucan in cancer. *Immunopharmacology* **1999**, *42*, 61-74.

(63) Maeda, Y. Y.; Chihara, G. Lentinan, a New Immuno-Accelerator of Cell-Mediated Responses. *Nature* **1971**, *229*, 634-&.

(64) Fujimoto, T.; Omote, K.; Mai, M.; Natsuumesakai, S. Evaluation of Basic Procedures for Adoptive Immunotherapy for Gastric-Cancer. *Biotherapy* **1992**, *5*, 153-163.

(65) Sonck, E.; Stuyven, E.; Goddeeris, B.; Cox, E. The effect of beta-glucans on porcine leukocytes. *Vet. Immunol. Immunopathol.* **2010**, *135*, 199-207.

(66) Hida, T. H.; Ishibashi, K.; Miura, N. N.; Adachi, Y.; Shirasu, Y.; Ohno, N. Cytokine induction by a linear 1,3-glucan, curdlan-oligo, in mouse leukocytes in vitro. *Inflammation Res.* **2009**, *58*, 9-14.

(67) Ljungman, A. G.; Leanderson, P.; Tagesson, C. (1 -> 3)-beta-D-glucan stimulates nitric oxide generation and cytokine mRNA expression in macrophages. *Environ. Toxicol. Pharmacol.* **1998**, *5*, 273-281.

(68) Kataoka, K.; Muta, T.; Yamazaki, S.; Takeshige, K. Activation of macrophages by linear (1 -> 3)-beta-D-glucans - Implications for the recognition of fungi by innate immunity. *J. Biol. Chem.* **2002**, *277*, 36825-36831.

(69) Xu, S.; Huo, J.; Lee, K.; Kurosaki, T.; Lam, K. Phospholipase C gamma 2 Is Critical for Dectin-1-mediated Ca2+ Flux and Cytokine Production in Dendritic Cells. *J. Biol. Chem.* **2009**, *284*, 7038-7046.

(70) Vetvicka, V.; Vetvickova, J.; Frank, J.; Yvin, J. Enhancing effects of new biological response modifier beta-1,3 glucan sulfate PS3 on immune reactions. *Biomed. Pharmacother.* **2008**, *62*, 283-288.

(71) Ohno, N.; Hashimoto, T.; Adachi, Y.; Yadomae, T. Conformation dependency of nitric oxide synthesis of murine peritoneal macrophages by beta-glucans in vitro. *Immunol. Lett.* **1996***, 52*, 1-7.

(72) Juul-Madsen, H. R.; Norup, L.; Laerke, H. N. Modulation of the immune response of porcine neutrophils by different beta-glucan preparations. *Livest. Sci.* **2010***, 133*, 249-252.

(73) Hamuro, J.; Chihara, G. Effect of Antitumor Polysaccharides on Higher Structure of Serum-Protein. *Nature* **1973***, 245*, 40-41.

(74) Maeda, Y. Y.; Chihara, G.; Ishimura, K. Unique Increase of Serum-Proteins and Action of Antitumor Polysaccharides. *Nature* **1974***, 252*, 250-252.

(75) Iino, K.; Ohno, N.; Suzuki, I.; Miyazaki, T.; Yadomae, T. Structural Characterization of a Neutral Antitumour Beta-D-Glucan Extracted with Hot Sodium-Hydroxide from Cultured Fruit Bodies of Grifola-Frondosa. *Carbohydr. Res.* **1985***, 141*, 111-119.

(76) Cheung, N. K. V.; Modak, S.; Vickers, A.; Knuckles, B. Orally administered beta-glucans enhance anti-tumor effects of monoclonal antibodies. *Cancer Immunol. Immunother.* **2002***, 51*, 557-564.

(77) Hamuro, J.; Yamashit.Y; Ohsaka, Y.; Maeda, Y. Y.; Chihara, G. Carboxymethylpachymaran, a New Water Soluble Polysaccharide with Marked Antitumour Activity. *Nature* **1971***, 233*, 486-&.

(78) Sasaki, T.; Abiko, N.; Nitta, K.; Takasuka, N.; Sugino, Y. Anti-Tumor Activity of Carboxymethylglucans obtained by Carboxymethylation of (1-]3)-Beta-D-Glucan from Alcaligenes-Faecalis Var Myxogenes Ifo-13140. *Eur. J. Cancer* **1979***, 15*, 211-215.

(79) Demleitner, S.; Kraus, J.; Franz, G. Synthesis and Antitumor-Activity of Sulfoalkyl Derivatives of Curdlan and Lichenan. *Carbohydr. Res.* **1992***, 226*, 247-252.

(80) Demleitner, S.; Kraus, J.; Franz, G. Synthesis and Antitumor-Activity of Derivatives of Curdlan and Lichenan Branched at C-6. *Carbohydr. Res.* **1992***, 226*, 239-246.

(81) Diluzio, N. R.; Williams, D. L. Protective Effect of Glucan Against Systemic Staphylococcus-Aureus Septicemia in Normal and Leukemic Mice. *Infect. Immun.* **1978***, 20*, 804-810.

(82) Wang, W. S.; Wang, D. H. Enhancement of the resistance of Tilapia and grass carp to experimental Aeromonas hydrophila and Edwardsiella tarda infections by several polysaccharides. *Comp. Immunol. Microbiol. Infect. Dis.* **1997***, 20*, 261-&.

(83) Dritz, S. S.; Shi, J.; Kielian, T. L.; Goodband, R. D.; Nelssen, J. L.; Tokach, M. D.; Chengappa, M. M.; Smith, J. E.; Blecha, F. Influence of Dietary Beta-Glucan on Growth-Performance, Nonspecific Immunity, and Resistance to Streptococcus-Suis Infection in Weanling Pigs. *J. Anim. Sci.* **1995***, 73*, 3341-3350.

(84) Eicher, S. D.; McKee, C. A.; Carroll, J. A.; Pajor, E. A. Supplemental, vitamin C and yeast cell wall beta-glucan as growth enhancers in newborn pigs and as immunomodulators after an endotoxin challenge after weaning. *J. Anim. Sci.* **2006***, 84*, 2352-2360.

(85) Li, J.; Li, D. F.; Xing, J. J.; Cheng, Z. B.; Lai, C. H. Effects of beta-glucan extracted from Saccharomyces cerevisiae on growth performance, and immunological and somatotropic responses of pigs challenged with Escherichia coli lipopolysaccharide. *J. Anim. Sci.* **2006**, *84*, 2374-2381.

(86) Stuyven, E.; Cox, E.; Vancaeneghem, S.; Arnouts, S.; Deprez, P.; Goddeeris, B. M. Effect of beta-glucans on an ETEC infection in piglets. *Vet. Immunol. Immunopathol.* **2009**, *128*, 60-66.

(87) Evans, S. G.; Morrison, D.; Kaneko, Y.; Havlik, I. The effect of curdlan sulphate on development in vitro of Plasmodium falciparum. *Trans. R. Soc. Trop. Med. Hyg.* **1998**, *92*, 87-89.

(88) Zhang, M.; Cheung, P. C. K.; Ooi, V. E. C.; Zhang, L. Evaluation of sulfated fungal beta-glucans from the sclerotium of Pleurotus tuber-regium as a potential water-soluble anti-viral agent. *Carbohydr. Res.* **2004**, *339*, 2297-2301.

(89) Yoshida, T.; Hatanaka, K.; Uryu, T.; Kaneko, Y.; Suzuki, E.; Miyano, H.; Mimura, T.; Yoshida, O.; Yamamoto, N. Synthesis and Structural-Analysis of Curdlan Sulfate with a Potent Inhibitory Effect Invitro of Aids Virus-Infection. *Macromolecules* **1990**, *23*, 3717-3722.

(90) Osawa, Z.; Morota, T.; Hatanaka, K.; Akaike, T.; Matsuzaki, K.; Nakashima, H.; Yamamoto, N.; Suzuki, E.; Miyano, H.; Mimura, T.; Kaneko, Y. Synthesis of Sulfated Derivatives of Curdlan and their Anti-Hiv Activity. *Carbohydr. Polym.* **1993**, *21*, 283-288.

(91) Yoshida, T.; Yasuda, Y.; Uryu, T.; Nakashima, H.; Yamamoto, N.; Mimura, T.; Kaneko, Y. Synthesis and In-Vitro Inhibitory Effect of L-Glycosyl-Branched Curdlan Sulfates on Aids Virus-Infection. *Macromolecules* **1994**, *27*, 6272-6276.

(92) TakedaHirokawa, N.; Neoh, L. P.; Akimoto, H.; Kaneko, H.; Hishikawa, T.; Sekigawa, I.; Hashimoto, H.; Hirose, S.; Murakami, T.; Yamamoto, N.; Mimura, T.; Kaneko, Y. Role of curdlan sulfate in the binding of HIV-1 gp120 to CD4 molecules and the production of gp120-mediated TNF-alpha. *Microbiol. Immunol.* **1997**, *41*, 741-745.

(93) Jeon, K. J.; Katsuraya, K.; Kaneko, Y.; Mimura, T.; Uryu, T. Studies on interaction mechanism of sulfated polysaccharides as an AIDS drug by NMR. *Macromolecules* **1997**, *30*, 1997-2001.

(94) Jagodzinski, P. P.; Wustner, J.; Kmieciak, D.; Wasik, T. J.; Fertala, A.; Sieron, A. L.; Takahashi, I.; Tsuji, T.; Mimura, T.; Fung, M. S.; Gorny, M. K.; Kloczewiak, M.; Kaneko, Y.; Kozbor, D. Role of the V2, V3, and CD4-binding domains of GP120 in curdlan sulfate neutralization sensitivity of HIV-1 during infection of T lymphocytes. *Virology* **1996**, *226*, 217-227.

(95) Jagodzinski, P. P.; Wiaderkiewicz, R.; Kurzawski, G.; Kloczewiak, M.; Nakashima, H.; Hyjek, E.; Yamamoto, N.; Uryu, T.; Kaneko, Y.; Posner, M. R.; Kozbor, D. Mechanism of the Inhibitory Effect of Curdlan Sulfate on Hiv-1 Infection In-Vitro. *Virology* **1994**, *202*, 735-745.

(96) Bagasra, O.; Lischner, H. W. Activity of Dextran Sulfate and Other Polyanionic Polysaccharides Against Human Immunodeficiency Virus. *J. Infect. Dis.* **1988**, *158*, 1084-1087.

(97) Naito, T.; Takeda-Hirokawa, N.; Kaneko, H.; Sekigawa, I.; Matsumoto, T.; Hashimoto, H.; Kaneko, Y. Role of curdlan sulfate in the production of beta-chemokines and interleukin-16. *Med. Microbiol. Immunol. (Berl.)* **1998**, *187*, 43-48.

(98) Gao, Y.; Fukuda, A.; Katsuraya, K.; Kaneko, Y.; Mimura, T.; Nakashima, H.; Uryu, T. Synthesis of regioselective substituted curdlan sulfates with medium molecular weights and their specific anti-HIV-1 activities. *Macromolecules* **1997**, *30*, 3224-3228.

(99) Gao, Y.; Katsuraya, K.; Kaneko, Y.; Mimura, T.; Nakashima, H.; Uryu, T. Synthesis, enzymatic hydrolysis, and anti-HIV activity of AZT-spacer-curdlan sulfates. *Macromolecules* **1999**, *32*, 8319-8324.

(100) Marchesan, S.; Da Ros, T.; Spalluto, G.; Balzarini, J.; Prato, M. Anti-HIV properties of cationic fullerene derivatives. *Bioorg. Med. Chem. Lett.* **2005**, *15*, 3615-3618.

(101) Ungurenasu, C.; Pinteala, M. Syntheses and characterization of water-soluble C-60-curdlan sulfates for biological applications. *J. Polym. Sci. Pol. Chem.* **2007**, *45*, 3124-3128.

(102) Hasegawa, T.; Umeda, M.; Numata, M.; Li, C.; Bae, A. H.; Fujisawa, T.; Haraguchi, S.; Sakurai, K.; Shinkai, S. 'Click chemistry' on polysaccharides: a convenient, general, and monitorable approach to develop (1 -> 3)-beta-D-glucans with various functional appendages. *Carbohydr. Res.* **2006**, *341*, 35-40.

(103) Hasegawa, T.; Umeda, M.; Numata, M.; Fujisawa, T.; Haraguchi, S.; Sakurai, K.; Shinkai, S. Click chemistry on curdlan: A regioselective and quantitative approach to develop artificial beta-1,3-glucans with various functional appendages. *Chem. Lett.* **2006**, *35*, 82-83.

(104) Borjihan, G.; Zhong, G. Y.; Baigude, H.; Nakashima, H.; Uryu, T. Synthesis and anti-HIV activity of 6-amino-6-deoxy-(1 -> 3)-beta-D-curdlan sulfate. *Polym. Adv. Technol.* **2003**, *14*, 326-329.

(105) Wong, S.; Ngiam, Z. R. J.; Kasapis, S.; Huang, D. Novel sulfation of curdlan assisted by ultrasonication. *Int. J. Biol. Macromol.* **2010**, *46*, 385-388.

(106) Browder, W.; Williams, D.; Lucore, P.; Pretus, H.; Jones, E.; Mcnamee, R. Effect of Enhanced Macrophage Function on Early Wound-Healing. *Surgery* **1988**, *104*, 224-230.

(107) Kougias, P.; Wei, D.; Rice, P. J.; Ensley, H. E.; Kalbfleisch, J.; Williams, D. L.; Browder, I. W. Normal human fibroblasts express pattern recognition receptors for fungal (1 -> 3)-beta-D-glucans. *Infect. Immun.* **2001**, *69*, 3933-3938.

(108) Delatte, S. J.; Evans, J.; Hebra, A.; Adamson, W.; Othersen, H. B.; Tagge, E. P. Effectiveness of beta-glucan collagen for treatment of partial-thickness burns in children. *J. Pediatr. Surg.* **2001**, *36*, 113-118.

(109) Williams, P. D.; Sadar, L. N.; Lo, Y. M. Texture Stability of Hydrogel Complex Containing Curdlan Gum Over Multiple Freeze-Thaw Cycles. *J. Food Process. Preserv.* **2009***, 33*, 126-139.

(110) Plahar, M. A.; Hung, Y.; McWatters, K. H. Improving the nutritional quality and maintaining consumption quality of akara using curdlan and composite flour. *Int. J. Food Sci. Technol.* **2006***, 41*, 962-972.

(111) Funami, T.; Yada, H.; Nakao, Y. Thermal and rheological properties of curdlan gel in minced pork gel. *Food Hydrocoll.* **1998***, 12*, 55-64.

(112) Funami, T.; Yada, H.; Nakao, Y. Curdlan properties for application in fat mimetics for meat products. *J. Food Sci.* **1998***, 63*, 283-287.

(113) Ferreira, D. S.; Faria, A. F.; Grosso, C. R. F.; Mercadante, A. Z. Encapsulation of Blackberry Anthocyanins by Thermal Gelation of Curdlan. *J. Braz. Chem. Soc.* **2009***, 20*, 1908-1915.

(114) Moon, C. J.; Lee, J. H. Use of curdlan and activated carbon composed adsorbents for heavy metal removal. *Process Biochem.* **2005***, 40*, 1279-1283.

(115) D'Cunha, N. J.; Misra, D.; Thompson, A. M. Experimental investigation of the applications of natural freezing and curdlan biopolymer for permeability modification to remediate DNAPL contaminated aquifers in Alaska. *Cold Reg. Sci. Technol.* **2009***, 59*, 42-50.

(116) Numata, M.; Asai, M.; Kaneko, K.; Hasegawa, T.; Fujita, N.; Kitada, Y.; Sakurai, K.; Shinkai, S. Curdlan and schizophyllan (beta-1,3-glucans) can entrap single-wall carbon nanotubes in their helical superstructure. *Chem. Lett.* **2004***, 33*, 232-233.

(117) Numata, M.; Sugikawa, K.; Kaneko, K.; Shinkai, S. Creation of hierarchical carbon nanotube assemblies through alternative packing of complementary semi-artiricial beta-1,3-glucan/carbon nanotube composites. *Chem. -Eur. J.* **2008***, 14*, 2398-2404.

(118) Dunstan, D. E.; Goodall, D. G. Terraced self assembled nano-structures from laminarin. *Int. J. Biol. Macromol.* **2007***, 40*, 362-366.

(119) Bae, A.; Numata, M.; Yamada, S.; Shinkai, S. New approach to preparing one-dimensional Au nanowires utilizing a helical structure constructed by schizophyllan. *New J. Chem.* **2007***, 31*, 618-622.

(120) Numata, M.; Li, C.; Bae, A. H.; Kaneko, K.; Kazuo, S. C.; Shinkai, S. beta-1,3-Glucan polysaccharide can act as a one-dimensional host to create novel silica nanofiber structures. *Chem. Commun.* **2005**, 4655-4657.

(121) Li, C.; Numata, M.; Hasegawa, T.; Fujisawa, T.; Haraguchi, S.; Sakurai, K.; Shinkai, S. Water-soluble poly(3,4-ethylenedioxythiophene) nanocomposites created by a templating effect of beta-1,3-glucan schizophyllan. *Chem. Lett.* **2005***, 34*, 1532-1533.

(122) Leung, T. C.; Wong, C. K.; Xie, Y. Green synthesis of silver nanoparticles using biopolymers, carboxymethylated-curdlan and fucoidan. *Mater. Chem. Phys.* **2010***, 121*, 402-405.

(123) Dobashi, T.; Nobe, M.; Yoshihara, H.; Yamamoto, T.; Konno, A. Liquid crystalline gel with refractive index gradient of curdlan. *Langmuir* **2004***, 20*, 6530-6534.

(124) Nobe, M.; Kuroda, N.; Dobashi, T.; Yamamoto, T.; Konno, A.; Nakata, M. Molecular weight effect on liquid crystalline gel formation of curdlan. *Biomacromolecules* **2005***, 6*, 3373-3379.

(125) Furusawa, K.; Minamisawa, Y.; Dobashi, T.; Yamamoto, T. Dynamics of liquid crystalline gelation of DNA. *J Phys Chem B* **2007***, 111*, 14423-14430.

(126) Dobashi, T.; Yoshihara, H.; Nobe, M.; Koike, M.; Yamamoto, T.; Konno, A. Liquid crystalline gel beads of curdlan. *Langmuir* **2005***, 21*, 2-4.

(127) Kanke, M.; Tanabe, E.; Katayama, H.; Koda, Y.; Yoshitomi, H. Application of Curdlan to Controlled Drug-Delivery .3. Drug-Release from Sustained-Release Suppositories In-Vitro. *Biol. Pharm. Bull.* **1995***, 18*, 1154-1158.

(128) Kanke, M.; Katayama, H.; Nakamura, M. Application of Curdlan to Controlled Drug-Delivery .2. In-Vitro and In-Vivo Drug-Release Studies of Theophylline-Containing Curdlan Tablets. *Biol. Pharm. Bull.* **1995***, 18*, 1104-1108.

(129) Kim, B. D.; Na, K.; Choi, H. K. Preparation and characterization of solid lipid nanoparticles (SLN) made of cacao butter and curdlan. *Eur. J. Pharm. Sci.* **2005***, 24*, 199-205.

(130) Subedi, R. K.; Kang, K. W.; Choi, H. Preparation and characterization of solid lipid nanoparticles loaded with doxorubicin. *Eur. J. Pharm. Sci.* **2009***, 37*, 508-513.

(131) Li, L.; Gao, F.; Tang, H.; Bai, Y.; Li, R.; Li, X.; Liu, L.; Wang, Y.; Zhang, Q. Self-assembled nanoparticles of cholesterol-conjugated carboxymethyl curdlan as a novel carrier of epirubicin. *Nanotechnology* **2010***, 21*, 265601.

(132) Kimura, T.; Koumoto, K.; Sakurai, K.; Shinkai, S. Polysaccharide-polynucleotide complexes (III): A novel interaction between the beta-1,3-glucan family and the single-stranded RNA poly(C). *Chem. Lett.* **2000**, 1242-1243.

(133) Koumoto, K.; Kimura, T.; Kobayashi, H.; Sakurai, K.; Shinkai, S. Chemical modification of curdlan to induce an interaction with poly(C)(1). *Chem. Lett.* **2001**, 908-909.

(134) Hasegawa, T.; Numata, M.; Okumura, S.; Kimura, T.; Sakurai, K.; Shinkai, S. Carbohydrate-appended curdlans as a new family of glycoclusters with binding properties both for a polynucleotide and lectins. *Org. Biomol. Chem.* **2007***, 5*, 2404-2412.

(135) Ikeda, M.; Hasegawa, T.; Numata, M.; Sugikawa, K.; Sakurai, K.; Fujiki, M.; Shinkai, S. Instantaneous inclusion of a polynucleotide and hydrophobic guest molecules into a helical core of cationic beta-1,3-glucan polysaccharide. *J. Am. Chem. Soc.* **2007***, 129*, 3979-3988.

(136) Numata, M.; Koumoto, K.; Mizu, M.; Sakurai, K.; Shinkai, S. Parallel vs. anti-parallel orientation in a curdlan/oligo(dA) complex as estimated by a FRET technique. *Org. Biomol. Chem.* **2005***, 3*, 2255-2261.

(137) Karinaga, R.; Anada, T.; Minari, J.; Mizu, M.; Koumoto, K.; Fukuda, J.; Nakazawa, K.; Hasegawa, T.; Numata, M.; Shinkai, S.; Sakurai, K. Galactose-PEG dual conjugation of beta-(1 -> 3)-D-glucan schizophyllan for antisense oligonucleotides delivery to enhance the cellular uptake. *Biomaterials* **2006***, 27*, 1626-1635.

(138) Karinaga, R.; Koumoto, K.; Mizu, M.; Anada, T.; Shinkai, S.; Sakurai, K. PEG-appended beta-(1 -> 3)-D-glucan schizophyllan to deliver antisense-oligonucleotides with avoiding lysosomal degradation. *Biomaterials* **2005***, 26*, 4866-4873.

(139) Dobashi, T.; Furusawa, K.; Kita, E.; Minamisawa, Y.; Yamamoto, T. DNA liquid-crystalline gel as adsorbent of carcinogenic agent. *Langmuir* **2007***, 23*, 1303-1306.

(140) Yoo, H. S.; Park, T. G. Biodegradable polymeric micelles composed of doxorubicin conjugated PLGA-PEG block copolymer. *J. Controlled Release* **2001***, 70*, 63-70.

(141) Gabizon, A.; Catane, R.; Uziely, B.; Kaufman, B.; Safra, T.; Cohen, R.; Martin, F.; Huang, A.; Barenholz, Y. Prolonged Circulation Time and Enhanced Accumulation in Malignant Exudates of Doxorubicin Encapsulated in Polyethylene-Glycol Coated Liposomes. *Cancer Res.* **1994***, 54*, 987-992.

(142) Zalipsky, S. Chemistry of Polyethylene-Glycol Conjugates with Biologically-Active Molecules. *Adv. Drug Deliv. Rev.* **1995***, 16*, 157-182.

(143) Gref, R.; Luck, M.; Quellec, P.; Marchand, M.; Dellacherie, E.; Harnisch, S.; Blunk, T.; Muller, R. H. 'Stealth' corona-core nanoparticles surface modified by polyethylene glycol (PEG): influences of the corona (PEG chain length and surface density) and of the core composition on phagocytic uptake and plasma protein adsorption. *Colloid Surf. B-Biointerfaces* **2000***, 18*, 301-313.

(144) Allen, T. M.; Cullis, P. R. Drug delivery systems: Entering the mainstream. *Science* **2004***, 303*, 1818-1822.

(145) Choi, Y. H.; Liu, F.; Kim, J. S.; Choi, Y. K.; Park, J. S.; Kim, S. W. Polyethylene glycol-grafted poly-L-lysine as polymeric gene carrier. *J. Controlled Release* **1998***, 54*, 39-48.